How to cite: *Angew. Chem. Int. Ed.* **2023,** *62,* e202216724
International Edition: doi.org/10.1002/anie.202216724
German Edition: doi.org/10.1002/ange.202216724

Water Treatment

Porous Materials for Water Purification

*Yanpei Song, Joshua Phipps, Changjia Zhu, and Shengqian Ma**

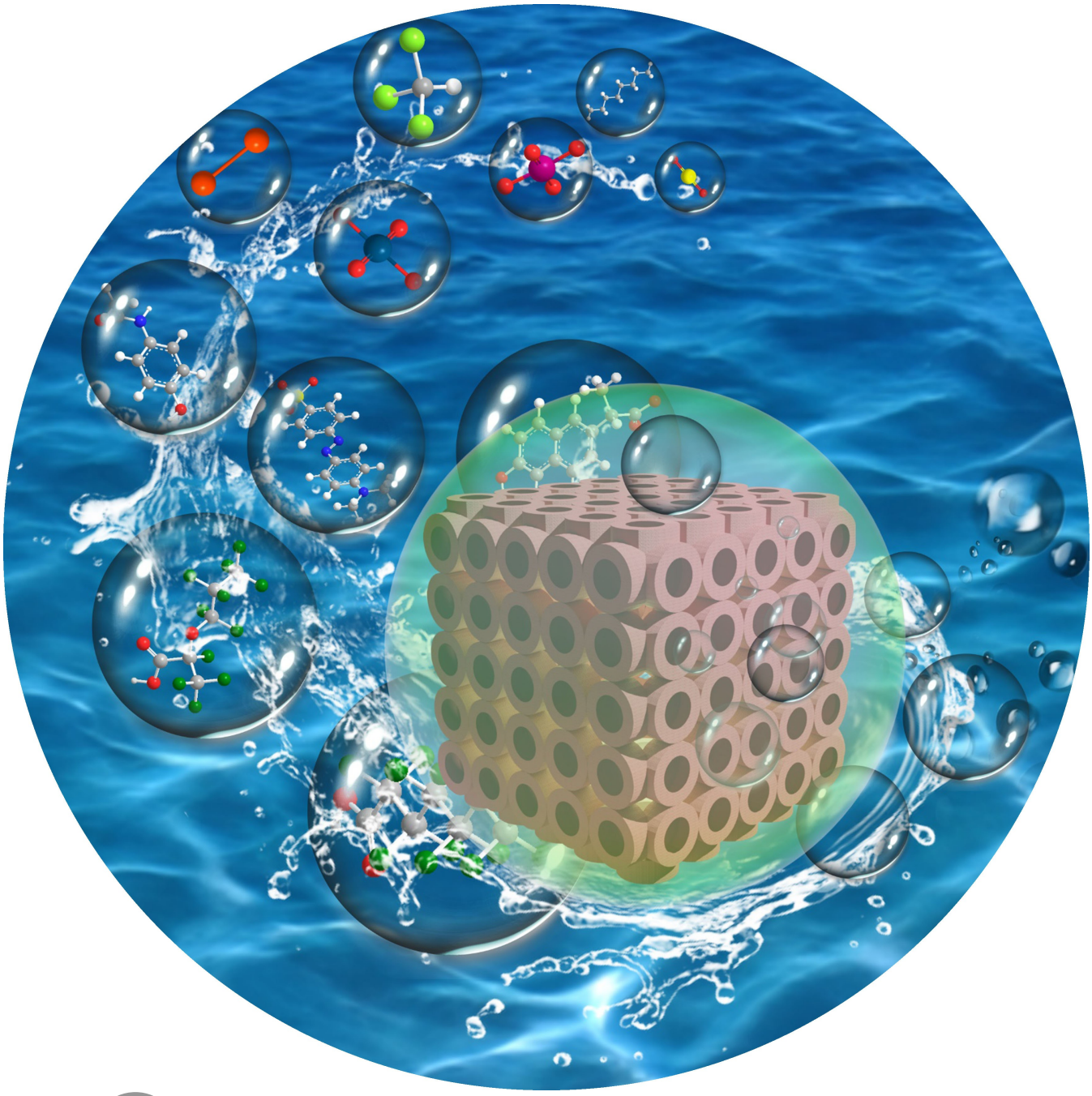

Angewandte International Edition Chemie

Abstract: Water pollution is a growing threat to humanity due to the pervasiveness of contaminants in water bodies. Significant efforts have been made to separate these hazardous components to purify polluted water through various methods. However, conventional remediation methods suffer from limitations such as low uptake capacity or selectivity, and current water quality standards cannot be met. Recently, advanced porous materials (APMs) have shown promise in improved segregation of contaminants compared to traditional porous materials in uptake capacity and selectivity. These materials feature merits of high surface area and versatile functionality, rendering them ideal platforms for the design of novel adsorbents. This Review summarizes the development and employment of APMs in a variety of water treatments accompanied by assessments of task-specific adsorption performance. Finally, we discuss our perspectives on future opportunities for APMs in water purification.

1. Introduction

Water is a renewable resource that is essential to all creatures on the earth; however, increasing water pollution caused by human activities, such as municipal domestic sewage, agricultural run-off, and industrial emission, seriously threatens global water security.[1] Therefore, the efficient elimination of contaminants present in water has become a great concern.[2] Conventional water purification methods including boiling, sedimentation, and distillation, are all associated with physical processes, which are convenient but limited in scope.[3] Recently, some chemical and biological processes have been utilized instead to oxidize the contaminations that cannot be removed conveniently as a supplement to physical water purification.[4] In addition, biological cleaning techniques are attracting much attention nowadays, including activated sludge,[4i] aerated lagoons,[4j] trickling filters,[4k] and rotating biological contactors.[4l] Nevertheless, these efforts to ameliorate water pollution have proven inadequate to redeem the rising water risks, given some stubborn water contaminants such as heavy metals[5] and trace organic contaminants (TrOCs)[6] which are still in desperate need of addressing, posing a great hazard to public health. Beyond the aforementioned strategies, adsorption is believed to be the best available technique for the efficient sequestration of trace contaminants from water supplies due to its affordable cost and high performance.[7] As the need for improved water quality rises, more advanced adsorbents with superior properties are called for to meet increasingly stringent water standards.

Porous materials housing permanent cavities in their structures are regarded as the ideal platform for the design of adsorbents.[8] Some traditional and well-known porous materials, such as porous carbons,[9] zeolites,[10] and mesoporous silica,[11] have long been explored as pollutant adsorbents and have shown a satisfactory capability to segregate contaminants from water. Recently, advanced porous materials (APMs), such as metal–organic frameworks (MOFs)[12] and covalent organic polymers (COPs) which include amorphous porous organic polymers (POPs)[13] and their crystalline relatives, covalent organic frameworks (COFs),[14] have been developed and have afforded us more opportunities to design task-specific adsorbents with stronger affinities compared with the conventional artificial porous materials.

MOFs are a kind of typical APM whose frameworks are built up via coordination bonds in a predictable manner, forming a crystalline network and allowing for the versatile manipulation of functional units and precise pore control that have increased the applicability of MOFs for water purification.[15] Crystalline COFs, being different from MOFs in that they are synthesized by purely organic monomers via more robust covalent bonds, also possess the benefit of easily functionalized building blocks and pore surfaces.[16] In addition to these, synthesized porous materials with purely organic backbones but lacking long-range order are usually identified as amorphous POPs.[17] Arising from their high porosity and unit tunability, any functional group can be grafted on the networks of these APMs in principle, giving MOFs and COPs the capacity for rapid recognition and capture of target contaminants.

Emerging trends in adsorption technology for sustainable water purification and freshwater supply protection have facilitated the fast development of APMs with versatile functions and the systematical study of the adsorption behaviors of given adsorbates on task-specific adsorbents. This Review summarizes the current trends in porous adsorbents for water purification and highlight the representative achievements in the research on APM-based adsorbents for various contaminant sequestration, as well as our outlook on the development of next-generation porous adsorbents. We hope to provide some useful suggestions for diminishing the threat to water quality in this Review.

2. Opportunities for APMs in Sustainable Water Purification

Due to the surplus of myriad organic reactions at a chemist's disposal, organic ligands/monomers can be functionalized by a large number of various moieties, thus providing the synthesized APMs with versatile functions to participate in a large number of applications. Because of this, APMs in many water treatment applications rely on specific interactions depending on the pollutant of choice. Usually, three different adsorption mechanisms are involved, according to the properties of contaminants: coordinative complexation, ion exchange, and host–guest interaction (Figure 1). To

[*] Y. Song, Dr. J. Phipps, C. Zhu, Prof. Dr. S. Ma
Department of Chemistry, University of North Texas
1508 W Mulberry St, Denton, TX 76201 (USA)
E-mail: shengqian.ma@unt.edu

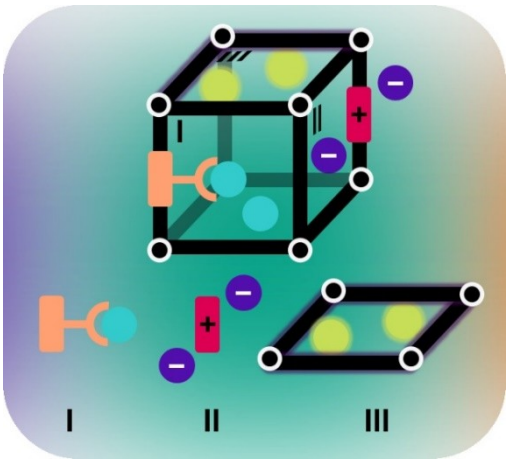

Figure 1. Three main adsorption mechanisms are involved during the design of APM absorbents for task-specific water purification: I. coordinative complexation, II. ion exchange, III. host–guest interactions.

ensure the highest degree of grafting of target adsorbents, the de novo synthetic strategy presents itself as an ideal candidate as it guarantees that each ligand/monomer unit contains a functional group. Alternatively, with the ease of functionalization of benzene rings existing in most polymers, a very high grafting of specified moieties can also be achieved via post-synthetic modification (PSM).[18] Besides placing functional groups in APM-based absorbents to achieve stated goals, MOFs and COFs that are arranged with long-range order provide an alternative strategy for the design of APMs for water purification. The entrance pore aperture of MOFs, referred to as the pore window, can be precisely controlled by the geometry of the linkers, affording them tailorable size sieving ability for small molecules. The pristine pore windows of MOFs are integrated into a wall which only allows for the free diffusion of molecules with a size smaller than the pore window, satisfying the prerequisite for the facile segregation of contaminants from water. Similar to MOFs, COFs also have significant advantages over amorphous POPs as advanced adsorbents. The cooperation between the open 1D pore channel present in 2D COFs and the pre-arranged binding groups on the surface of the pore wall can facilitate the transport of analytes and strengthen the interaction between adsorbents and targeted species,[19] thus improving adsorption performance. Taking advantage of these benefits provided by APMs, a variety of water purification systems can be constructed with tailored porous materials.

3. Water Purification

Depending on the chemical constituents of compounds found in water, contaminants can be divided into two subclasses: inorganic and organic. For instance, heavy metal pollution is a notorious water quality issue primarily due to the discharge of inorganic metals from industry. These can

Yanpei Song received his B.S. degree from Beijing University of Chemical Technology in 2017. He is currently a Ph.D. candidate under the supervision of Prof. Shengqian Ma in the Department of Chemistry, University of North Texas. His current research interests lie primarily in the development of functional porous organic polymers for environmental remediation and precious metal recovery.

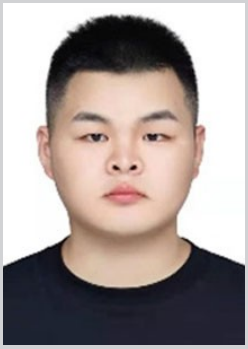

Changjia Zhu received his B.S. degree from University of Science and Technology of China in 2020. He then worked for one year as a research assistant at Zhejiang University before starting his M.S. career with Prof. Shengqian Ma at the University of North Texas. His research focuses on the development of covalent organic framework membranes for environmental remediation and precious metal recovery.

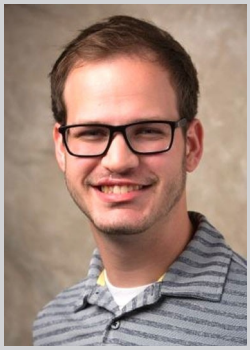

Joshua Phipps received his B.S. degree in biology from Southwest Baptist University, Bolivar (USA) in 2017 and his PhD in Cell and Molecular Biology from the University of Arkansas in Fayetteville in 2022. He currently works as a postdoctoral researcher under the supervision of Prof. Shengqian Ma in the Department of Chemistry, University of North Texas. His research focuses on the interactions between porous and biological materials as well the development of new drug delivery methods and catalytic techniques.

Shengqian Ma obtained his B.S. degree from Jilin University (China) in 2003, and graduated from Miami University (Ohio, USA) with a PhD degree in 2008. After finishing a two-year Director's Postdoctoral Fellowship at Argonne National Laboratory, he joined the Department of Chemistry at University of South Florida as an Assistant Professor in 2010; he was promoted to Associate Professor with early tenure in 2015 and to Full Professor in 2018. In August 2020, he joined University of North Texas as the Robert A. Welch Chair in Chemistry. His current research interest focuses on the task-specific design and functionalization of advanced porous materials for energy-, biological-, and environmental-related applications.

be highly toxic and carcinogenic, posing a significant risk to public health. Furthermore, various organic pollutants have also been globally detected in water supplies including drinking water at trace concentrations and originate mainly from industrial activities and increasing use of plastic products. The sharp accumulation of these hazardous compounds in human bodies stemming from exposure to contaminated water can result in adverse health effects, significantly increasing the risks of many diseases. Thus, continuous efforts for addressing such hazards are urgently needed. APMs demonstrate promising potential in the prevention of this unfortunate outcome, though there is still a long way to go before the practical employment of large-scale APMs in real water purification.

3.1. Dye Removal

The use of dyes has a long history, and it is believed that the blue dye indigo was one of the first organic dyes used nearly 4000 years ago.[20] With the rising demand for colorful textiles and clothing at an affordable price due to the ever-growing population, artificial dyes has become prevalent in modern industry and have substantially lowered the cost of pigmentation technology. It is estimated that over 700000 tons of synthetic dyes are consumed per year and more than 10000 different dyes are available on the market today.[21] Currently, a considerable amount of untreated dye effluents is discharged into surface water and the quantity of these waste dyes accounts for over 15% of dyes produced annually. Due to their robust chemical structure, dyes are difficult to decompose/degrade after entering water bodies. These stubborn dyes will eventually mix into domestic water, which can lead to a wide array of serious health effects.[22]

Given the high surface areas, rich pore structures, and possibilities in the functionalization of APMs, all MOFs, COFs, and POPs demonstrate promising application for dye separation from the water supply. Technologically, there are two approaches available for the successful segregation of dyes from water. First, the dye molecules present in water can be rejected through the use of a sophisticated membrane. Meanwhile, the small water molecules can penetrate the membranes, thus achieving water purification. This type of membrane liquid-separation technology for dye removal is called nanofiltration (NF), which typically relies on size exclusion. The second approach is based on the highly selective adsorption of dye molecules in porous particles, which requires careful selection and deliberate functionalization of solid-phase adsorbents.

MOFs bearing appropriate pore windows between 0.3 and >10 nm in size are most suitable for NF. Their inherent crystalline nature indicates that the pore window of the majority of MOFs is persistent, suggesting that selective molecular sieving through MOF membranes can be achieved effortlessly in principle. In 2009, Basu and co-workers reported the successful application of mixed matrix membranes (MMMs) with MOFs for high retention of organic dyes.[23] However, the prepared MMMs were incontinuous and defective until Zhang et al. presented an accessible strategy for the preparation of continuous and defect-free MOF hybrid membranes which was named coordination-driven in situ self-assembly.[24] In this work, the synthesized ZIF-8/PSS membrane was obtained by pouring a solution of 2-methylimidazole and poly(sodium 4-styrenesulfonate) (PSS) into a Zn^{+}-loaded polyacrylonitrile (PAN) that had been placed in a dead-end filtration cell under negative pressure. Then, the removal of methyl blue (MB) from water using this ZIF-8/PSS membrane was evaluated, revealing that 98.6% of MB could be retained with a flux of 265 $L\,m^{-2}h^{-1}MPa^{-1}$ under optimal conditions. The study also stressed the close relationship between the molecular size of the dye and its retention with the ZIF-8/PSS membrane, supporting the theory that the NF of dyes was primarily based on size exclusion. Cohen and co-workers also contributed a lot to the preparation of processable MOF MMMs; the facile approach they developed allowed for a wide range of MOFs to be blended with polymers to fabricate MMMs with a high MOF content (Figure 2).[25] A typical example of these MOF–polymer composite membranes is UiO-66 MMMs which have been employed to purify water spiked with various organic dyes and showed the effective removal of dye from the solution.

Because of the flexibility of monomer selection and the diversity of covalent bonds, it is possible to fine-tune the apertures of POPs in line with requirements. This is especially true when using COFs, which possess ordered pore channels and uniform pore structures. Banerjee and

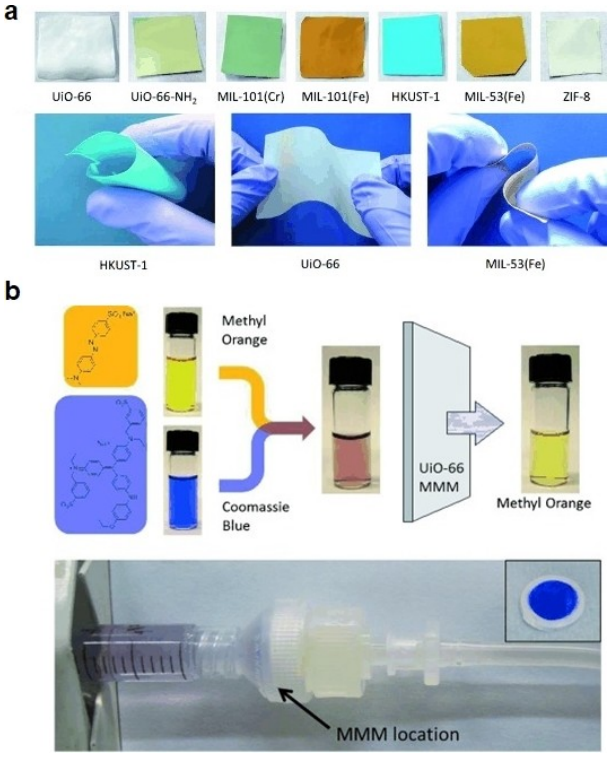

Figure 2. a) Photographs of free-standing MMMs produced from a variety of MOFs. b) Aqueous dye sequestration with UiO-66 MMM. Reproduced with permission.[25] Copyright 2015, Wiley-VCH.

co-workers proposed an elegant methodology for the preparation of self-standing, defect-free, and crystalline COF membranes (COMs) with high flexibility (Figure 3).[26] In this work, the authors used *p*-toluene sulfonic acid (PTSA) as the catalyst which served as the binder of aldehyde and amine monomers, and also acted as a water reservoir for the Schiff base reaction. A library of COMs was also showcased in this report, and permeation experiments were conducted to assess the permeation and rejection of organic matter using these NF membranes. The reported results suggested that the dye molecules with molecular dimensions above 1 nm could be completely rejected due to the uniform micropores within these COMs, indicative of their capacity for water purification in textile/dye industries. In addition to this, the molecular sieving ability of COF membranes can be promoted by adjusting the charge properties of the framework. Given that a large number of dye molecules are charged, Ma and co-workers prepared a thin cationic COF membrane, namely EB-COF:Br, via the interfacial polymerization of a cationic monomer, ethidium bromide (EB), and 1,3,5-triformylphloroglucinol (TFP), in order to achieve better rejection of positively charged dyes.[27] The thin films formed at the liquid–liquid interface were then stacked by a layer-by-layer process to obtain continuous, large-scale, and dense EB-COF:Br membranes with controlled thickness, further increasing their applicability for water treatment. Due to the size exclusion effect and electrostatic interactions between charged pore walls and dye ions, the synthesized cationic membrane demonstrated remarkable retention of the anionic dyes fluorescein sodium salt (FSs), methyl orange (MO), and potassium permanganate (PP) of up to 99.2 %, 99.6 %, and 98.1 %, respectively. However, lower rejection values of cationic and neutral dyes were reported using the same membrane under identical conditions, revealing the excellent selective molecular sieving performance of EB-COF:Br membrane.

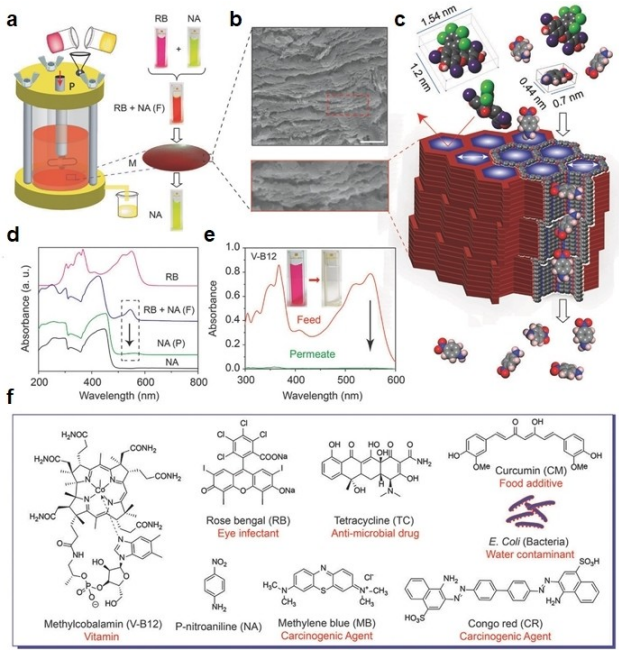

Figure 3. a) Schematic representation of the nanofiltration assembly and selective molecular separation of NA from a mixture of NA and RB. b) SEM cross-section showing stacked layered sheets of M-TpBD (scale bar 10 μm). c) Schematic representing the molecular sieving mechanism of M-TpBD. d) UV-vis spectra of selective recovery of NA from a mixture of RB and NA in water. e) UV/Vis spectra of vitamin B12 and the water filtrate after passing through M-TpBD. f) A library of dye molecules, active pharmaceuticals, and *E. coli* bacteria used for nanofiltration experiments using COMs. Reproduced with permission.[26] Copyright 2016, Wiley-VCH.

While membrane separation technology for dye removal from wastewater has distinguished itself as a topic of interest, the development of new adsorbents to eliminate dye pollution has also recently garnered much attention. The ultrahigh chemical/hydrolytic stability of COPs due to their purely organic backbones allows for their application in a wide range of chemical conditions and make them especially suitable for complex water treatment. Although MOFs typically have lower stability than COPs when present in water, these novel porous materials with remarkably large surface areas, adjustable porosity, and tailored functionalities also have significant implications for adsorption applications,[28] including its gas adsorption as well as use for pollutant sorption from water. Feasible solid-phase adsorbents for dye removal should satisfy the demands of rapid adsorption rate, high extraction uptake, and easy recycling, which requires abundant active sites for efficient encapsulation of diverse dye molecules/ions. Haque et al. recently developed a dense iron terephthalate with a cationic framework, namely MOF-235, for the efficient removal of not only an anionic dye (MO) but also a cationic dye (MB).[29] A zirconium-metalloporphyrin mesoMOF (PCN-222) with dual functions of large pore size and suitable zeta potentials which would affect the interaction and the adsorption capacity was selected by Li and co-workers for the removal of MO and MB, as well.[30] PCN-222, also called MOF-545, has a high Brunauer–Emmett–Teller (BET) surface area of 2336 $m^2 g^{-1}$ and a large open channel with a diameter of 3.7 nm, while the MOF is microporous (pore size <2 nm), making it suitable for holding organic dye molecules in the "nanopockets". Besides, the zeta potentials of PCN-222 ranging from 23.5 mV at pH 3 to −13.6 mV at pH 10 exhibited relatively large positive and negative potentials, affording PCN-222 the ability to adsorb both cationic and anionic dyes in solution. The high extraction capacity for MB (1239 $mg g^{-1}$) and MO (1022 $mg g^{-1}$) was achieved, respectively, revealing the significance of the cooperation of high porosity, aligned active sites, and suitable zeta potentials during the adsorption process.

2D COFs with abundantly accessible 1D channels are also widely utilized for dye removal. Apart from the more common MB and MO, rhodamine B (RhB) is another toxic dye that poses a high carcinogenic risk after entering human bodies.[31] Two COFs (TPT-azine-COF and TPT-TAPB-COF) both supported by a heteroatom-rich linker TPT-CHO and various amine monomers were tested for RhB removal (Figure 4a).[32] The high efficiencies of RhB removal

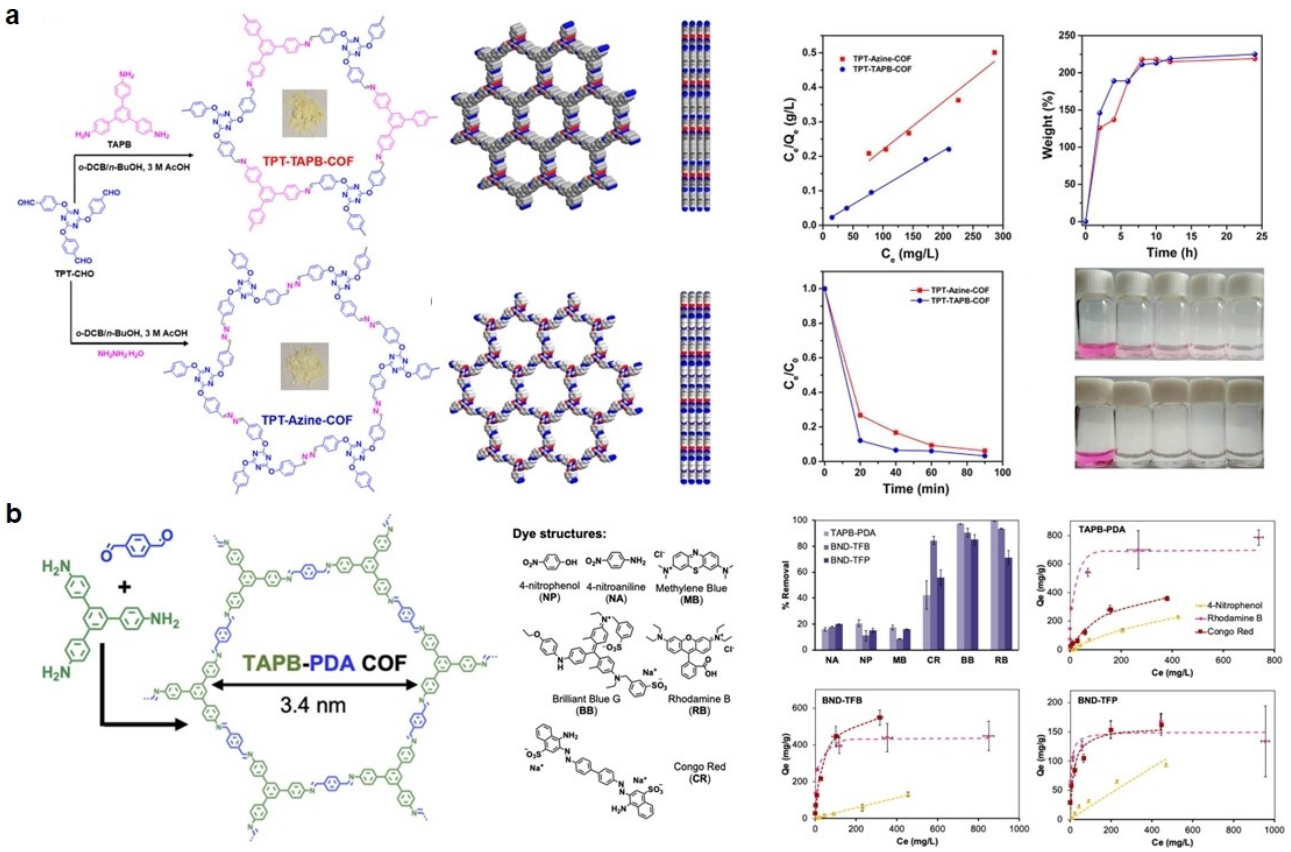

Figure 4. Examples of COFs used for dye removal. a) Synthesis of the TPT-COFs and their adsorption performance for RhB. Reproduced with permission.[32] Copyright 2018, American Chemical Society. b) Synthesis of the TAPB-PDA COF and its capacity for removing various organic dyes. Reproduced with permission.[33] Copyright 2021, American Chemical Society.

of TPT-azine-COF ($725\ mg\,g^{-1}$) and TPT-TAPB-COF ($970\ mg\,g^{-1}$) were recorded during the RhB adsorption experiments; the results were in line with their BET surface areas ($957\ m^2\,g^{-1}$ and $1020\ m^2\,g^{-1}$ for TPT-TAPB-COF and TPT-azine-COF, respectively). Interestingly, Dichtel and co-workers reported a polycrystalline COF film that acted as an adsorbent instead of a membrane for dye elimination from water (Figure 4b).[33] To do this, they compressed 100 mg of TAPB-PDA COF powder between two polyester discs to produce a COF pellet that could be mounted for flow studies. The resulting disc-shaped COF pellet would swell and quadruple in thickness (from ≈350 to ≈1300 μm) without cracking when a small amount of water passed through it. When a continuous flow of RhB solution was passed through the prewetted COF pellet, a decreased rejection rate of RhB was reported as the whole COF pellet changed color with the collection of RhB, thus, indicating that the adsorption mechanism successfully facilitated the dye removal from the water flow. Amorphous POPs with tailored functionalization also possess the ability to retain water-soluble organic dyes in their pores.[34] However, their extraction capacity is typically lower than that of COFs due to their disordered rigid polymeric backbone which can obstruct the accessibility of dyes entering the pore space.

3.2. Oil-Spill Cleanup

Oil leakage from crude oil extraction and transportation is a growing concern worldwide, threatening the global ecosystem. It is estimated that over 10 billion dollars is spent on oil-spill cleanup all over the world annually.[8b] The old-fashioned technologies used for oil-spill cleanup, such as centrifugation and in situ burning, are costly, have low efficiency, and introduce the possibility of secondary pollution. To lower the cost, traditional adsorbents including active carbon, zeolites, and sand, have been used for water purification after an oil spill. However, these adsorbents tend to absorb water and other dissolved components besides oil, sharply compromising their performance for oil-spill cleanup. Thus, developing novel adsorbents for the selective capture of organic liquids from water is an urgent need in environment control. To this end, improving material hydrophobicity has been proposed as a general approach to solving the problem associated with water absorptivity, and APM-based adsorbents have been extensively studied in this task-specific field (Table S1).

Our group has conducted some significant research on the wettability of APMs. We developed a porphyrin-based POP (PCPF-1) through the homocoupling of 5,10,15,20-tetrakis(4-bromophenyl)porphyrin (tbpp).[35] The combination of the 2D layered structure, exposed conjugated

porphyrin, and phenyl rings in the resulting POP produces a high surface area with strong hydrophobicity, affording PCPF-1 the capacity for selective extraction of petroleum oil from a water mixture. Saturated C5–C8 hydrocarbons and gasoline were chosen to assess its adsorption performance. In this test, an extraordinarily high gasoline uptake capacity (20.5 $g\,g^{-1}$) was observed; PCPF-1 outperformed all reported POPs at that time, showing its great potential for use in oil-spill cleanup. However, PCPF-1 powder is produced by a cumbersome synthesis and is not easily recycled in real-world applications. In addition to this, its limited pore volume also encumbers its adsorption capabilities. Thus, to address these concerns, we also reported the employment of function-specific COFs in the cleanup of oil spills from water (Figure 5).[36] To do this, we devised a facile approach to endow COF-V with superhydrophobicity by engineering the pore surface. This is demonstrated by the chemical modification of the exterior of a vinyl-functionalized COF with fluorinated compounds via a thiol–ene click reaction to afford COF-VF. From this, we creatively integrated the COF-VF with commercial melamine foams, yielding an affordable superhydrophobic foam (COF-VF@foam). To realize the homogeneous distribution of the COF throughout the foam, we first submerged the monolithic melamine foam in a solution of two monomers, 1,3,5-tris(4-aminophenyl)-benzene and 2,5-divinylterephthalaldehyde, and then added the catalyst (acetic acid). This resulted in the in situ coating of COF-V on the melamine foam. Next, the modified foam was treated with 1*H*,1*H*,2*H*,2*H*-perfluorodecanethiol to graft the perfluoroalkyl groups to the pore surface of COF-V to yield COF-VF@foam. The uptake performance of the resulting COF-VF@foam was examined with multiple organic liquids afterward. Owing to its superhydrophobicity and superoleophilicity, sorption capacities from 67 to 142 times its weight were achieved, suggesting a wide broad applicability of COF-VF@foam for oil-spill cleanup. What's more, using the foam as the support to load COF-VF results in adsorbent good recyclability, since the captured oil can be simply squeezed out. Because of this, the spent COF-VF@foam could be immediately regenerated for adsorption without a significant loss in its performance for at least ten cycles, stressing the superiority of COFs compared to POPs for the design of advanced adsorbents for oil-spill cleanup.

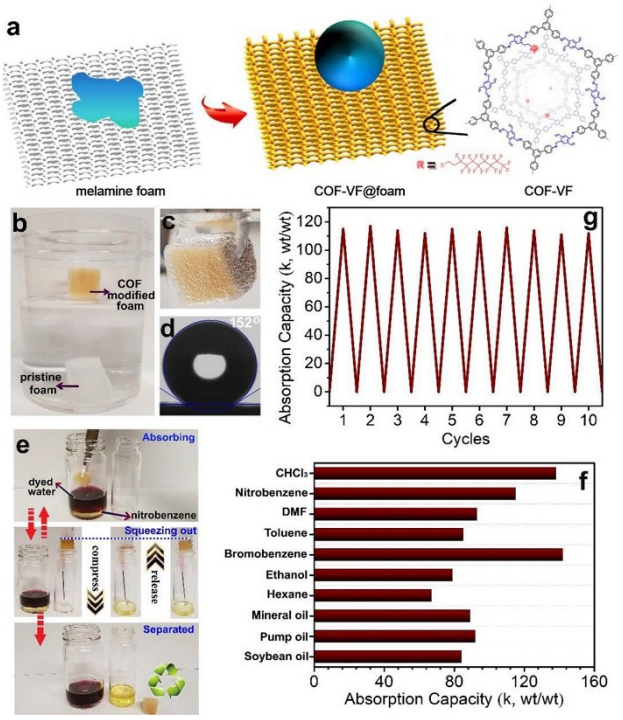

Figure 5. a) Schematic illustration of the preparation of superhydrophobic COF-VF coated melamine foam (COF-VF@foam). b) Photograph of COF-VF@foam and melamine foam after introduction to water. c) Photograph of COF-VF@foam immersed in water. d) Water contact angle on the surface of COF-VF@foam. e) Illustration of the ability of submerged COF-VF@foam to separate nitrobenzene from water. f) Absorption capacities of COF-VF@foam in the presence of various organic solvents and oils, as indicated by weight gain. g) Weight gain during nitrobenzene absorption/squeezing cycles. Reproduced with permission.[36] Copyright 2018, Elsevier.

Another type of functional porous polymer, conjugated microporous polymers (CMPs), has recently been revealed as a promising tool for applications in oil–water separation by the rational design of porosities and lipophilic networks. Li and co-workers presented a successful case of constructing the surface superhydrophobicity of CMPs for the first time and used the resulting CMPs for oil adsorption from water.[37] Their CMP, known as HCMP-1, was synthesized from 1,3,5-triethynylbenzene via homocoupling polymerization, while an analog of HCMP-1 was produced from binary monomers, 1,3,5-triethynylbenzene and 1,4-diethynylbenzene. Both HCMPs demonstrated a large water contact angle (CA) of 167° and 157° for HCMP-1 and HCMP-2, respectively, and were also strongly oleophilic due to their superhydrophobicity and open pore structures. These merits allowed for the resulting HCMPs to selectively capture oil and nonpolar organic solvents with fast adsorption kinetics. For HCMP-1, a maximum absorbency for oils that reached up to 10 times its weight was observed, as well as excellent adsorption for various organic solvents that ranged from approximately 700 wt % to 1500 wt %. To improve the functionality for large-scale removal of toxic organic pollutants, an HCMP-1 treated sponge was also produced by simply immersing a sponge into a chloroform solution of HCMP-1. The final sponge coated with HCMP-1 was endowed with hydrophilic and oleophilic properties, and could absorb 0.6 and 0.9 tons of octane and nitrobenzene per cubic meter of the as-treated sponge, respectively. Du et al. utilized a freeze-drying synthesis technique to obtain CMP aerogels to construct hierarchical pore structures in the resulting adsorbents, which significantly accelerated the matter transfer in pores (Figure 6).[38] The adsorption of diverse organic solvents and oils was evaluated using CMP aerogel and the corresponding CMP network. Higher absorbencies ranging from 20 to 53 times its weight were showcased for the CMP aerogel, while the CMP network displayed sorption capacities of only 1 to 16 times its weight, illustrating the significance of hierarchically porous structures in adsorbents for pollutant removal.

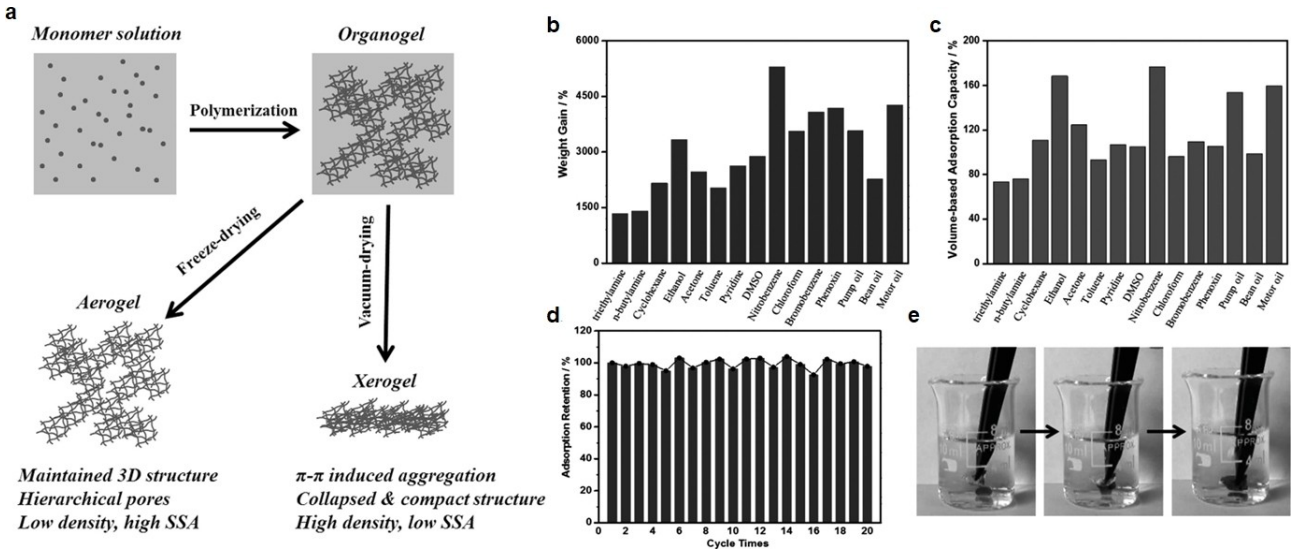

Figure 6. a) Schematic illustration of preparation and structure of the PTEB aerogel and xerogel. Mass-based (b) and volume-based (c) adsorption capacity of the PTEB aerogel. d) Adsorption-capacity retention of the PTEB aerogel toward acetone through regeneration by heating at 60 °C for 20 cycles. e) Demonstration of uptake of chloroform (containing Sudan III dye) under water, by using a piece of PTEB aerogel. Reproduced with permission.[38] Copyright 2014, Wiley-VCH.

The wettability of MOFs can also be readily manipulated by functional moiety design and surface morphology control.[39] The first report on the adsorption of typical aromatic and aliphatic oil components using fluorous metal–organic frameworks (FMOFs) whose pore surface is fluorine-lined and hydrogen-free was presented by Yang et al. in 2011.[40] The synthesized FMOF-1, which was constructed from silver(I) 3,5-bis(trifluoromethyl)-1,2,4 triazolate (AgTz), revealed its great capacity for oil-spill cleanup due to its hydrophobic pore surface. Later, one of the most well-known MOFs, HKUST-1, was also utilized for oil removal from water (Figure 7a).[41] Its oil removal ability was tested in a milky aqueous solution containing in an emulsion of 300 mg L^{-1}. After the emulsion containing a dispersion of HKUST-1 had been shaken vigorously, a clear solution could be observed when the adsorption was finished. The maximal removal capacity of HKUST-1 was estimated up to 4000 mg g^{-1} according to the Langmuir isotherm model. To improve the uptake capacity of MOFs for organic oils, significant efforts were made to grow MOFs on a variety of supports. A considerable number of hydrophobic MOF-based sponges/foams were developed for water purification from oil-in-water emulsions. For comparison, the oil uptake capacity of FG-HKUST-1 sponge was increased to over 8000 mg g^{-1} (Figure 7b),[42] which was about two times higher than that of pristine HKUST-1 mentioned above. Moreover, Yang and co-workers employed a modified melamine foam with a 2D MOF (kgd-Zn), called kgd-Zn@MF, for application in oil-spill cleanup;[43] it showed a high adsorption capacity (5077—13786 wt %) towards various solvents and oils, which was comparable with the COF-coated melamine foams (for a summary of the oil sorption performance of various APM-based adsorbents, see Table S1).

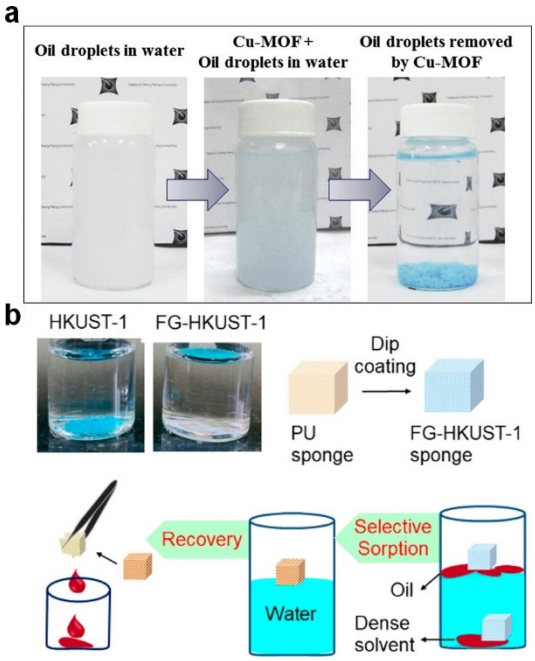

Figure 7. Application of the HKUST-1 family in oil adsorption. a) Photographs showing the oil droplets being removed from water by HKUST-MOF. Reproduced with permission.[41] Copyright 2014, Elsevier. b) Schematic representation of FG-HKUST-1 composite's hydrophobicity, solution processability, and selective oil sorption from an oil–water mixture and oil recovery. Reproduced with permission.[42] Copyright 2020, American Chemical Society.

3.3. Treatment of Trace Organic Contaminants

In addition to the above organic pollutants, the contamination of water systems by TrOCs is also prevalent in freshwater bodies. These pollutants are mainly produced by

urban discharge, agricultural production, and industrial processes. Although TrOCs are detected in low concentrations ranging from the ppt (one part per trillion) to ppb (one part per billion) level in surface water, sufficient evidence has emerged to prove that even a low concentration of TrOCs will threaten human health with prolonged ingestion. In the past decades, various physicochemical and biological treatments have been devoted to segregating TrOCs from freshwater,[44] but most TrOCs are difficult to deal with and their removal by these conventional water purification methods has been inefficient. APMs, with their excellent adsorption–desorption properties, are well suited for the efficient removal of hazardous TrOCs.[45] What's more, the unique tunability of structures and functions in APMs enables advanced oxidation reactions in water, such as the Fenton reaction, photolysis, photocatalysis, ozonation etc., which have been reported extensively for the degradation of a variety of TrOCs.

Perfluorinated and polyfluorinated alkyl substances (PFAS), which include perfluorooctanoic acid (PFOA) and perfluorooctanesulfonic acid (PFOS), are a typical class of TrOCs found today. These are widely utilized in food packaging, fire-fighting foams, household products, and in many industrial plants due to their durability.[46] The outstanding durability, however, is also their pitfall. These "forever chemicals" cannot be biodegraded in nature and will accumulate in living organisms once introduced into the environment. Prolonged exposure to PFAS can cause the onset of illnesses including cancer, thyroid conditions, kidney disease, and autoimmune disease.[47] Because of this, the development of highly efficient adsorbents for the rapid capture of trace PFAS from water with a strong binding is urgently needed.

Given the unique host–guest interaction and well-defined intrinsic porosities of *β*-cyclodextrin (*β*-CD) and other kinds of macrocycles, it is possible to implant these functional units into porous organic polymers to enhance their capture performance for PFAS.[48] Dichtel and co-workers have become pioneers in this new field of advanced porous material design;[49] and have presented the very first example of *β*-CD-based POPs for the rapid removal of PFAS from water.[49a] To accomplish this, the researchers crosslinked *β*-cyclodextrin with rigid aromatic groups to form mesoporous polymers, integrating *β*-CD's special affinity toward these contaminants into the porous networks. The BET surface area of the as-prepared DFB-CDP was less than 10 $m^2 g^{-1}$; however, the material allowed 95 % of PFOA to be removed from the water solution, while the PFOA concentration in the treated water sample was decreased from 1 $\mu g L^{-1}$ to 20 $ng L^{-1}$ within 24 h, which was lower than the U.S. Environmental Protection Agency (EPA) limit of 70 $ng L^{-1}$ at that time. In contrast, their previously reported porous *β*-CD-based polymer with a high surface area (263 $m^2 g^{-1}$), called P-CDP, lacked the capacity for PFOA removal ($\approx$0 %), even though it demonstrated an unparalleled extraction performance for organic contaminants like bisphenol A (BPA) (Figure 8).[49b] To better understand the adsorption mechanisms of *β*-CD-based polymers and to develop more efficient adsorbents, Dichtel

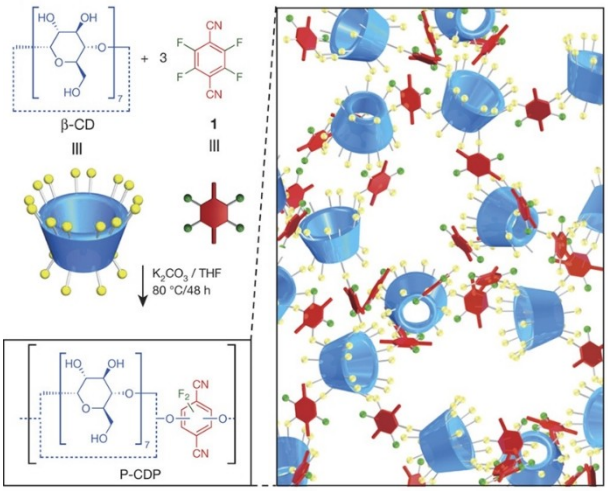

Figure 8. Left: Synthesis of the high-surface-area porous P-CDP from β-CD and **1**. Right: Schematic of the P-CDP structure. Reproduced with permission.[49b] Copyright 2015, Springer Nature.

and co-workers have also reported a library of modified CDPs devoted to PFAS removal.[49c–f] One example from this list comes from TFN-CDP in which the nitrile groups were reduced to primary amines in order to improve its affinity toward anionic organic contaminants and stronger binding to anionic PFAS.[49c] The PFAS removal performance and adsorption kinetics of the modified TFN-CDP were examined in PFAS-spiked water with a concentration of 1 $\mu g L^{-1}$. The resulting data showed that the combined concentration of PFOA and PFOS was rapidly reduced to 58 $ng L^{-1}$ after 30 min contact with the amine-functionalized TFN-CDP.

COFs constructed by the linkage of NH_2-*β*-CD and aldehyde monomers have also been developed recently. Wang et al. selected terephthalaldehyde (TPA) as the joint knots to connect heptakis(6-amino-6-deoxy)-*β*-CD (Am7CD) to construct the framework of *β*-CD COFs.[50] The COF produced exhibited highly selective adsorption for a broad range of TrOCs in water, such as BPA, ibuprofen, naproxen, and 4-nonyl phenol. Later, the application of this type of COF in PFAS removal was also studied by Deng and co-workers (Figure 9),[51] revealing the superior extraction capacity of *β*-CD COFs for PFAS compared to traditional adsorbents (e.g., resins and activated carbons). Furthermore, a comprehensive adsorption study of thirteen different PFAS molecules using amine-functionalized 2D-COFs was conducted by Dichtel and co-workers.[52] In this study, 1,3,5-tris(4-aminophenyl)benzene with the mixture of TPA and dialdehyde bearing azide-functionalized ethylene glycol side chains was used to synthesize azide-functionalized COFs. Next, the azide groups in the resulting COFs were reduced by using PPh_3 to afford X%[NH_3]-COFs where X ranges from 0 to 100 %. Ammonium perfluoro-2-propoxypropionate (GenX) was then selected to evaluate the adsorption performance of [NH_3]-COFs containing various densities of amine groups. A COF with 20 % amine loading showed the highest uptake of GenX among all

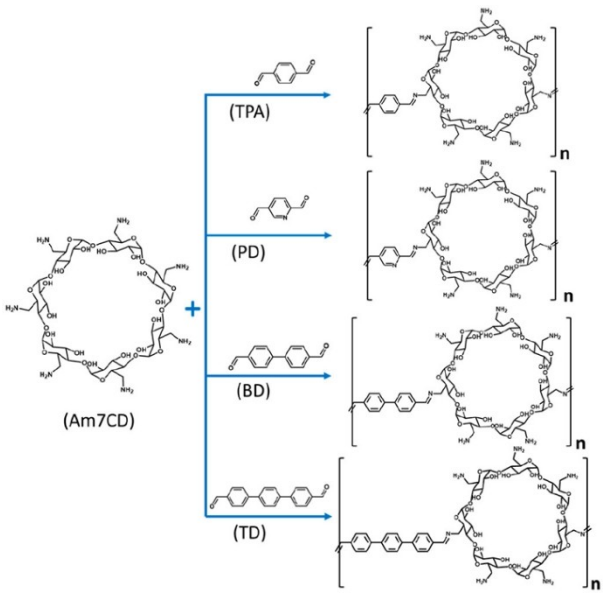

Figure 9. Synthesis of β-CD COFs including COF1, COF2, COF3, and COF1N. Reproduced with permission.[51] Copyright 2021, American Chemical Society.

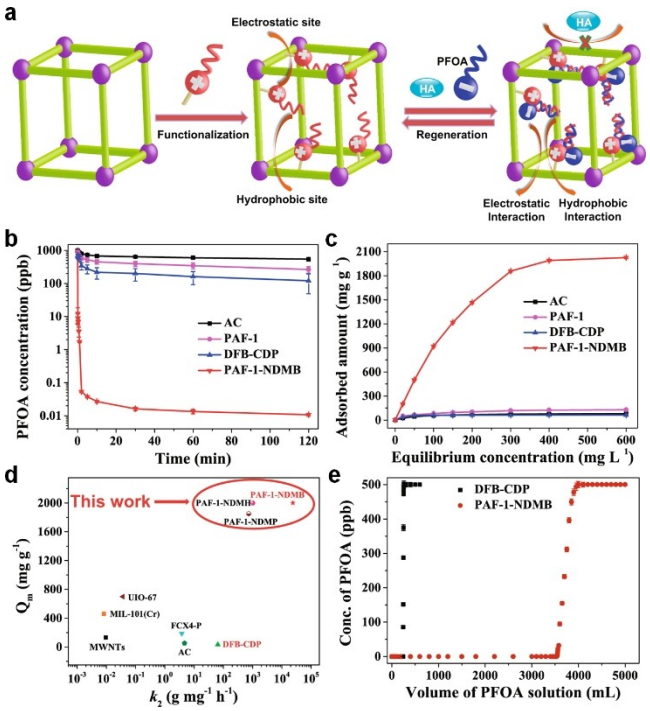

Figure 10. a) Illustration of the "synergistic binding sites" strategy to construct highly efficient sorbents for PFOA removal. b) PFOA sorption kinetics of AC, PAF-1, DFB-CDP, and PAF-1-NDMB. c) Plot of equilibrium PFOA adsorption capacity as a function of equilibrium PFOA concentration. d) Comparison of PFOA saturation uptake amounts and k_2 values for PAF-1-NDMB with other threshold porous materials, including DFB-CDP, MIL-101(Cr), MWNTs, FCX4-P, UIO-67, and AC. e) Breakthrough experiments for PAF-1-NDMB and DFB-CDP in aqueous PFOA/HA solutions (PFOA 500 ppb, HA 20 ppm). Reproduced with permission.[53] Copyright 2022, Springer Nature.

functional COFs, while 28 %[NH_3]-COF had the broadest applicability for PFAS removal, achieving adsorption of more than 90 % in 12 out of 13 PFAS tested.

Ma and co-workers presented a facile strategy to apply a porous aromatic framework (PAF) with task-specific modification for the rapid removal of PFOA from water (Figure 10a).[53] Using this method, three hydrophobic chains with varying lengths functionalized with quaternary ammonium groups were successfully appended to the framework of PAF-1, yielding PAF-1-NDMB, PAF-1-NDMP, and PAF-1-NDMH. The performance of these functionalized PAF-1 adsorbents was assessed by their effectiveness in extracting PFOA from water solutions. PAF-1-NDMB exhibited an optimal sorption performance compared to the other two PAF-1 derivatives: 99.99 % removal of PFOA could be achieved by PAF-1-NDMB within 2 min. with a remarkable reduction in PFOA concentration from 1000 ppb to 54 ppt. The saturated uptake capacity of PAF-1-NDMB was also estimated from the adsorption to be 2000 mg g^{-1} at the equilibrium concentration of 600 ppm, surpassing all benchmark materials at the time. Following this, the practical application of PAF-1-NDMB in water purification was investigated in a breakthrough experiment using a 500 ppb PFOA water solution (Figure 10b). The results showed that 3530 mL of water contaminated by PFOA could be purified to drinking-water standards (< 53 ppt) with only 300 mg adsorbent added. For comparison, only 242 mL potable water (62 ppt) could be produced by the same mass of DFB-CDP, displaying the superiority of PAF-1-NDMB for the removal of PFAS from polluted water.

Crystalline MOFs exhibit promising adsorption performance for PFAS, as well. Li et al. proved this when they selected several well-studied MOFs with different pore sizes/shapes and chemical constitutions, for a comprehensive survey of various PFAS removal.[54] Liu et al. also introduced a family of quaternary and tertiary amine-functionalized MIL-101(Cr) and their application in PFOA adsorption.[55] Depending on the PSM method, various amine groups were grafted on the surface of MIL-101(Cr); the optimal adsorption capacity for PFOA was recorded with a value as high as 1.89 mmol g^{-1}. Apart from the introduction of basic units to MOFs to enhance their adsorption performance, another factor that can affect PFOS adsorption is the control of the cavity size present in MOFs. Sini et al. stated this when they selected two zirconium MOFs, UiO-66 and UiO-67, to test this assumption.[56] UiO-67 bearing a larger cavity is built up by biphenyl-dicarboxylic acid (bpdc), while a shorter ligand, benzene-dicarboxylic acid (bdc) is applied in the construction of UiO-66. The change of sorption mechanism as the result of the increased cavity size was observed in UiO-67 and led to a higher sorption capacity of PFOA for UiO-67 (743 mg g^{-1}) compared to UiO-66 (388 mg g^{-1}). Furthermore, using MOFs for the photocatalytic degradation of PFAS has also been investigated very recently. Zhou and co-workers reported a titanium-based MOF, namely MIL-125-NH_2, which can degrade over 98.9 % PFOA under Hg-lamp irradiation in 24 h benefiting from the coordinated contribu-

tion of hydrated electron (e_{aq}^-) and light-induced hydroxyl radical (•OH) from MIL-125-NH_2.[57]

In addition to the previously mentioned organic contaminants, another environmental risk that is presently increasing is the presence of trace residual pharmaceuticals and personal care products (PPCPs) and endocrine-disrupting chemicals in water. These contaminants threaten the aquatic ecosystem and cause adverse human health impacts via biomagnification, where contaminants make their way up the food chain. Adsorption has become a promising technology to eliminate the effects of these invisible organic contaminants due to its low cost, high efficiency, and sustainability. Using MOFs as an alternative in the sorption of PPCPs from water has become popular because of their characteristic porosity. This is especially true for the MOF UiO and MIL series,[58] which have been widely applied in the removal of PPCPs including acetaminophen (ACE), amoxicillin (AMX), carbamazepine (CBZ), ciprofloxacin (CPX), sodium diclofenac (DCF), ketoprofen (KTP), naproxen (NPX), and other related contaminants. As a prime example, Lin et al. recently presented that UiO-66 had high adsorption capacities for IBU and KTP of up to 606.49 mg g^{-1}, and 638.24 mg g^{-1}, respectively.[59]

Given their high surface areas and large pore channels, COFs also excel in the adsorption of PPCPs. Zhuang et al. introduced the application of TPB-DMTP-COF for the removal of sulfamerazine (SMT) from water, achieving a high extraction capacity of 209 mg g^{-1} together with a fast adsorption equilibrium and good recyclability.[60] Wen et al. also developed a spherical COF (TPB-DMTP-COF) that provides an advancement for the testing of sulfonamides in water and food.[61] These are a class of chemically synthesized antibacterial drugs and are widely used in animal feed to prevent diseases. The resulting spherical COF was mounted in the SPE (solid-phase extraction) column to test its effectiveness in detecting trace-level sulfonamides in dairy products and exhibited broad applicability for various sulfonamides (SAs) including sulfadiazine (SD), sulfapyridine (SP), sulfathiazole (ST), sulfamerazine (SM_1), sulfamethazine (SM_2), and sulfamethoxazole (SMX). Another development direction has been that of magnetic COFs. These are similar in nature to other COFs but can be easily separated, and are ideal materials for the removal of pharmaceutical pollutants from water. Huang and co-workers applied TFP, *p*-phenylenediamine (PDA), and –NH_2-functionalized Fe_3O_4@SiO_2 nanoparticles (MNP-NH_2) as basic building units to construct the magnetic COFs (MCOFs).[62] The tailored MCOF-2 with its high crystallinity and high surface area combined with excellent chemical/thermal stability was tested for the removal of DCF, a nonsteroidal anti-inflammatory drug, from water supplies. The results showed a high uptake capacity (565 mg g^{-1}) for DCF, outcompeting well-known adsorbents, such as UiO-66 (189 mg g^{-1}) and ZIF-8 PCDM-1000 (360 mg g^{-1}). Ma and co-workers also reported the application of porous organic frameworks in the rapid and efficient capture of ofloxacin, one of the most common antibiotics (Figure 11).[63] In contrast to 3D COFs, the 3D porous oligomer frameworks that were reported in this work were self-assembled through collaborative intermolecular hydrogen bonding, endowing them flexible pore structures and open channels for encapsulating larger organic molecules. The performance of ofloxacin extraction was evaluated using HOF-TAM-BDA and the corresponding COF material (COF-320), revealing that HOF-TAM-BDA had a fast initial adsorption rate up to 140.92 mg g^{-1} min^{-1}, while a much slower rate of

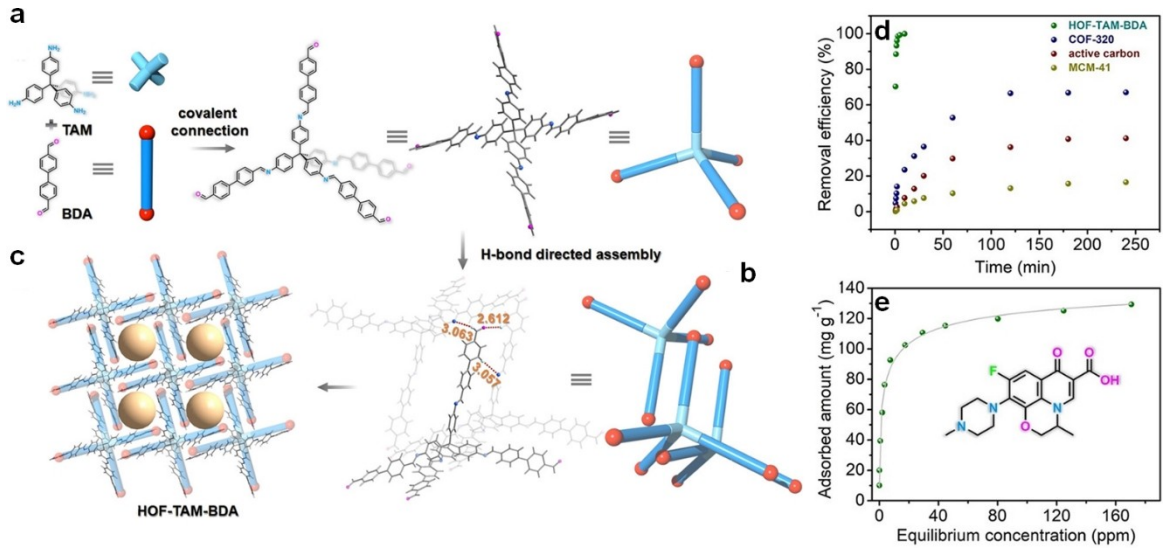

Figure 11. a) Synthesis of the oligomer constructed for HOF-TAM-BDA. b, c) X-ray crystal structure of HOF-TAM-BDA featuring multiple hydrogen bonds (red dashed lines) between adjacent units to form a 3D framework exhibiting quasi square-shaped pores with a diameter of about 10.6 Å along the *c* axis. Length of hydrogen bonds in Å. For clarity, only hydrogen atoms that have hydrogen bonding interactions with the guest molecule are shown (C gray, N blue, O magenta, H light cyan). d) Ofloxacin sorption kinetics of various porous materials with an initial ofloxacin concentration of 20 ppm at a V m^{-1} ratio of 1 mL mg^{-1}. e) Ofloxacin adsorption isotherm for HOF-TAM-BDA. Inset: chemical structure of ofloxacin. Reproduced with permission.[63] Copyright 2021, Wiley-VCH.

$0.95\ mg\,g^{-1}\,min^{-1}$ was observed in COF-320. Additionally, the maximum adsorption capacity of HOF-TAM-BDA was determined to be $151.5\ mg\,g^{-1}$ with excellent recyclability.

APMs have been shown to act not only as selective adsorbents of contaminants but also as task-specific catalysts for the degradation of organic pollutants through advanced oxidation. The first example of this function was reported using MOF-5 as a photocatalyst to degrade methyl viologen dichloride in water.[64] Following this, a considerable amount of related work has been published on the subject in the past decade. Recently, Gómez-Avilés et al. proposed a set of mixed Ti–Zr MOFs and displayed their employment as photocatalysts in the ACE oxidation under solar-simulated radiation.[65] The authors obtained these MOFs through the partial substitution of Ti by Zr atoms in the crystalline structure of NH_2-MIL-125(Ti) MOF. The catalytic performance was determined to be controlled by the adjustment of the Ti:Zr molar ratio, showing that lower Zr loading in the treated MOFs with retained crystalline structure had high activity for the photocatalytic degradation of ACE. The optimized mixed MOF, TiZr15, demonstrated the highest activity in photocatalytic degradation, allowing for complete ACE conversion after only 90 min. During the catalytic process, $O_2^{\bullet-}$ radicals are detected and identified as the main reactive species. Meanwhile, the photogenerated $^{\bullet}OH$ radicals and electrons also were identified as playing significant roles in the degradation of organic contaminants. The sulfate radicals ($^{\bullet}SO_4^-$) generated by these MOFs were also explored for the degradation of TrOCs, and are commonly used in the oxidation of pesticides (atrazine, malathion, and 2,4-dichlorophenoxyacetic acid) and antibiotics (tetracycline, sulfamethoxazole, and sulfamethoxazole).[66] Yin et al. took a representative Fe-MOF, MIL-100(Fe), for the study of peroxydisulfate activation and its potential for the removal of antibiotics.[67] Under irradiation, the surface Fe^{III} on the structure would be reduced to Fe^{II}, which would cause the formation of $^{\bullet}SO_4^-$. The generated $^{\bullet}SO_4^-$ would then promote the generation of $^{\bullet}OH$ and $O_2^{\bullet-}$ radicals, which would act directly in the degradation of antibiotics.

COPs, such as COFs and CMPs with extended π-conjugated structures, also contribute to water purification via the efficient degradation of TrOCs. Very recently, Dong et al. proposed a strategy to load single Cu sites in the COF to enhance its photocatalytic performance (Figure 12).[68] The as-prepared COF-909 contains abundant terpyridyl-based units, providing open triple coordinative bonding to transitional metals, such as Cu. Due to the unique COF chemical structure, Cu can be easily loaded to COF-909 to form COF-909(Cu) by simply soaking the COF material in copper chloride-methanol solution without heating for 12 h. The photocatalytic activity of the resulting COF was examined for the degradation of SMX with or without visible-light irradiation. It was reported that more than 98 % of SMX could be eliminated within 30 min when the light was on, while no obvious concentration change of SMX could be detected in the same period under identical conditions without light, suggesting that light is indispensable to the generation of reactive oxygen species (ROS) by COF-909(Cu). The modification of COFs with active metal sites is also reported in porphyrin-based COFs. Hou et al. obtained a copper porphyrin-based COF through the condensation of 5,10,15,20-tetra(*p*-aminophenyl)-porphyrinato copper (CuTAPP) with TPA on the surface of g-C_3N_4.[69] The 2D porphyrin COF/g-C_3N_4 heterostructure in the resulting CuPor-Ph-COF/g-C_3N_4 not only increases the visible light absorption of the material but also accelerates its charge carrier transport, which promises excellent photocatalytic performance for degrading organic contaminants. This strategy of integrating metal with the porphyrin units in

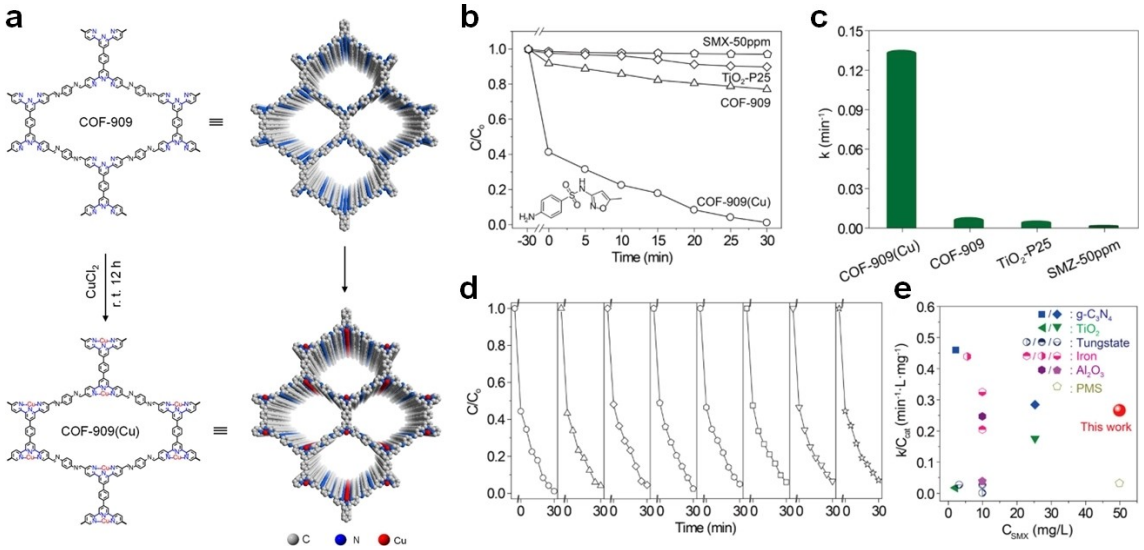

Figure 12. a) Synthesis of COF-909(Cu) nanorods. b) Efficiency of SMX removal using COF-909(Cu), COF-909, or TiO_2-P25; the inset shows the chemical structure of SMX. c) Pseudo-first-order kinetic constants of COF-909(Cu), COF-909 and TiO_2-P25 in the degradation of SMX. d) Recyclability of COF-909(Cu) for the photocatalytic degradation of SMX. e) Comparison of COF-909(Cu) with state-of-the-art photocatalysts. Reproduced with permission.[68] Copyright 2021, Elsevier.

the porous networks is also employed in the construction of CMPs with active metal site loading. Xiao et al. developed a UPC-CMP-1 with highly efficient and selective photocatalytic ability via a Sonogashira–Hagihara coupling reaction between iron(III) 5,10,15,20-tetrakis-(4-bromophenyl)-porphyrin and 1,4-diethynylbenzene, which demonstrated fast and selective decomposition of Congo red over other dye molecules.[70] The authors also made a significant discovery in that the degradation efficiency of metal porphyrin-based CMPs could be regulated by changing the type of metal sites in the porphyrin units, and thereby tailoring CMPs with specific and improved photocatalytic performance becomes possible.

3.4. Elimination of Heavy Metals

Heavy metal pollution is currently one of the most prevalent environmental issues and is harmful not only to aquatic life but also to human beings. Toxic heavy metal ions present in surface water, such as Hg^{II}, Pb^{II}, Cr^{VI}, As^{III}, As^{V}, and Cu^{II}, which mostly come from the discharge of industrial wastewater, are increasing the risks of public health problems and threatening biological systems as the tolerance levels are exceeded. For example, high levels of lead can damage the central nervous system in humans and affect children's brain development, resulting in reduced intelligence quotient (IQ). Similarly, prolonged exposure to mercury will also lead to serious damage of the nervous system (e.g., Minamata disease), as well as other diseases, such as neurological or behavioral disorders and cancer. Damage to other organs (e.g., lung, kidney, and liver) can be directly linked to drinking water containing hexavalent chromium over extended time. To eliminate these adverse health impacts brought by heavy metals, many methods have been developed for the removal of these ions.[71] These methods include chemical precipitation, ion exchange, membrane filtration, and adsorption. Recently, a considerable amount of APMs have been employed as novel adsorbents for removing heavy metal ions.

To implement an APM as a task-specific nanotrap, their functional groups must be carefully tailored to meet the demand. Ma and co-workers developed a series of PAF-based nanotraps that were utilized in the efficient sorption of metal ions by the installation of diverse chelators in PAF-1. For mercury removal, PAF-1 was modified with a thiol group, which has a strong affinity toward mercury ions and exceptional mercury binding capacity (Figure 13).[72] To obtain the target PAF-based nanotrap, PAF-1 was first treated with concentrated HCl to complete the chloromethylation. The resulting PAF-1-CH_2Cl was then reacted with NaHS to finish the thiol conversion. The final product, PAF-1-SH, showed an exceptional maximum mercury uptake capacity of over 1000 $mg\,g^{-1}$ (at an equilibrium concentration of $\approx$800 ppm) and an extraordinary distribution coefficient (K_d) value of $5.76\times10^7\,mL\,g^{-1}$ combined with outstanding adsorption kinetics. These results demonstrated that the Hg^{II} concentration could be reduced from 10 ppm to an extremely low level of 0.4 ppb after treatment with

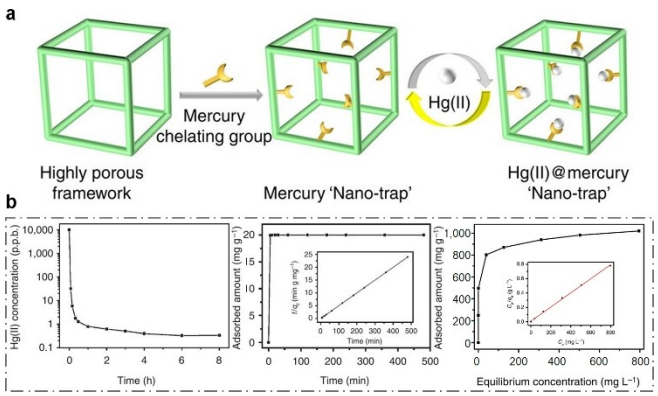

Figure 13. a) Illustration of creating a mercury "nano-trap" for Hg^{II} removal from water. b) Kinetics and adsorption capacity investigation for PAF-1-SH. Reproduced with permission.[72] Copyright 2014, Springer Nature.

PAF-1-SH, which surpasses the acceptable limits set by the EPA for drinking water (2 ppb). In addition, PAF-1-SH retained a high adsorption performance for Hg^{II} not only in the solutions with a wide pH range of 3–11, but also in complex systems with high concentrations of background metal ions, such as Na^{I}, Mg^{II}, Zn^{II}, and Ca^{II}.

However, the synthetic procedures required to construct PAF-1-SH hinder its practical application; thus a more economically feasible synthesis is necessary for the development of a POP-based adsorbent with refined application and accessibility. To solve this problem, Ma and co-workers, using the experience gained from the previous work, advanced a more feasible method for synthesizing mercury nanotraps.[73] A monomer unit incorporated with a chloromethyl group was used for the polymerization of POPs, which has shown promise as a higher grafting of chelators in the resulting polymer. To prepare this thiol-functionalized POP, 3,5-divinylbenzyl chloride first underwent free-radical polymerization with azobisisobutyronitrile (AIBN). Next, the resulting POP was treated with NaHs and the chloride moiety was replaced by the thiol group, which gave the thiol-functionalized polymer, POP-SH. This amorphous material has a high BET surface area of 1061 $m^2\,g^{-1}$ and a broad distribution of pore sizes, indicating the presence of hierarchical porosity in POP-SH that can offer high accessibility to the chelating sites. The maximum mercury saturation uptake capacity of POP-SH was found to be 1216 $mg\,g^{-1}$ (at an equilibrium concentration of $\approx$200 ppm), showing a sorption performance comparable to that of many state-of-the-art mercury adsorbents (for a summary of the Hg^{2+} sorption performance of various sorbent materials, see Table S2). In addition to removing mercury from water samples, POP-SH was also capable of mercury vapor adsorption with an uptake capacity of 630 $mg\,g^{-1}$. However, X-ray absorption fine structure (XAFS) spectra collected for Hg-loaded POP-SH demonstrated a multimodal distribution of Hg–S distances, indicative of distinct Hg–S scattering paths, which is primarily the result of inefficient cooperation of the binding sites present in amorphous material with a rigid polymeric backbone.

To address this shortcoming in POPs that might obstruct sorption performance, COF was chosen as the decorating platform providing an ordered structure with excellent cooperation towards chelators. The 2D COF, COF-V, was then designed as a support to graft various thiol and thioether chelating arms via thiol–ene "click" reactions (Figure 14).[74] Record-setting adsorption capacities for Hg^{II} in aqueous solutions and Hg^0 in the gas phase were obtained up to 1350 (at an equilibrium concentration of ≈100 ppm) and 863 mg g^{-1}, respectively, which confirmed our assumption that anchored chelators oriented in the same direction would facilitate greater binding affinity between the adsorbates of interest and corresponding chelators. Ding et al. also proposed a thioether-functionalized COF via a de novo synthesis by using a thioether monomer (2,5-bis(3-(ethylthio)propoxy)terephthalohydrazide) as the building block.[75] The resulting COF-LZU8 was exploited as a sensor for the real-time detection of Hg^{II} ions, as well as an efficient adsorbent, which could reduce the mercury concentration from 10 ppm to less than 0.2 ppm in 3 hours. A library of MOFs decorated by thiol and thioether groups has also been developed for mercury elimination.[76] To the best of our knowledge, Zr-MSA, which was synthesized by using mercaptosuccinic acid (MSA) as the ligand, had the best adsorption capacity (734 mg g^{-1}) for Hg^{II} in water among all sulfurized MOF materials.[77] Apart from capturing mercury, the thioether-functionalized APMs have also been shown to be effective in copper removal. Lee et al. reported the employment of a PAF-based material, PAF-1-SMe, in the selective extraction of copper ions with a maximum capacity of over 600 mg g^{-1}.[78]

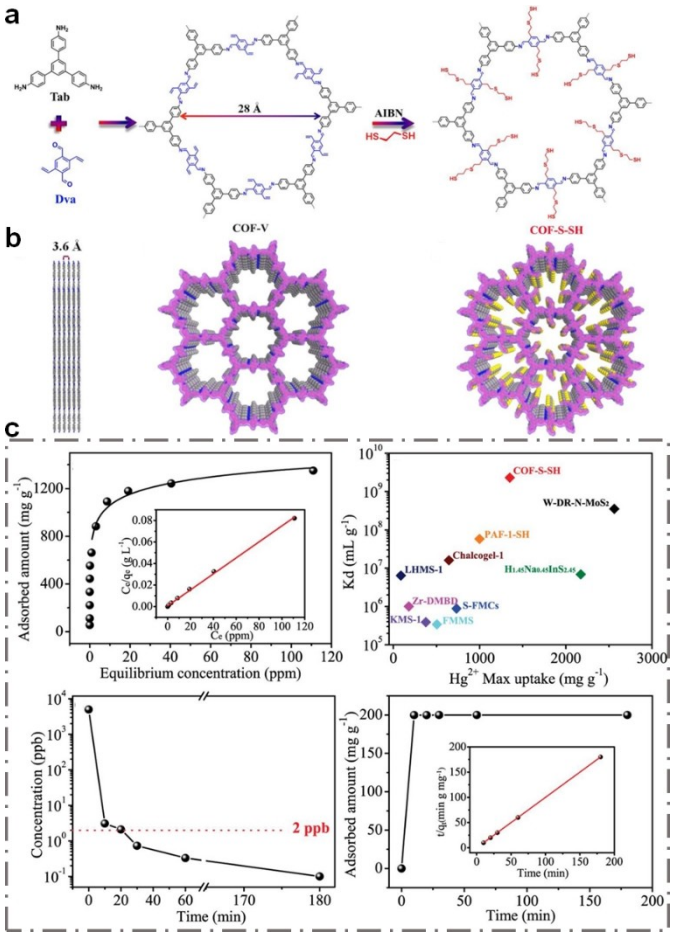

Figure 14. a) Synthesis of COF-V and representative channel-wall engineering by thiol–ene reaction with (COF-S-SH). b) Graphic view of the slipped AA stacking structure of COF-V (blue, N; gray, C; hydrogen is omitted for clarity) and a graphic view of COF-S-SH (N blue, C gray, S yellow; hydrogen is omitted for clarity). c) Hg^{2+} adsorption performance for COF-S-SH. Reproduced with permission.[74] Copyright 2017, American Chemical Society.

Cr^{III} and Cr^{VI} are the most stable and predominant forms of chromium, and Cr^{III} ions specifically are considered nontoxic. In contrast, Cr^{VI} is noxious and carcinogenic. Numerous efforts have been made to eliminate Cr^{VI} oxoanions from water in the past. However, with the development of APMs, a promising new route to solve this problem has arrived. Toward this end, Zhao and co-workers reported the efficient removal of Cr^{VI} using novel dual-pore COFs bearing hydroxyl groups.[79] The resulting COF, COF-BTA-DHBZ, demonstrated rapid adsorption of Cr^{VI} in aqueous solutions (272 mg g^{-1} within 10 min), and showed a saturated adsorption capacity of up to 384 mg g^{-1}. Cationic POPs have also been studied for the improved removal of Cr^{VI} through ion exchange.[80] For example, Ma and co-workers showcased the application of an imidazolium-based 3D cationic POP for the efficient collection of Cr^{VI} from wastewater.[81] Furthermore, with Cr^{III} ions being nonhazardous, the reduction of Cr^{VI} to Cr^{III} has been proposed as another common method to eliminate the threat caused by Cr^{VI} and as such, a variety of MOFs having photocatalytic abilities have been exploited in this area. For instance, a 2D Zn-MOF synthesized from pamoic acid, 4,4′-bipyridine, and $Zn(ClO_4)_2 \cdot 6H_2O$ exhibited a promising photocatalytic reduction of Cr^{VI} to Cr^{III};[82] starting from an initial Cr^{VI} concentration in solution of 20 ppm, nearly all (>99 %) Cr^{VI} ions could be reduced to trivalent chromium within 90 min.

3.5. Radionuclide Sequestration

Nuclear energy is considered an alternative to fossil fuels which is capable of meeting global energy and environmental needs. However, the inadvertent release of radioactive materials into the environment poses potential health risks to human beings. Various radionuclides can be detected in nuclear wastewater, with unreacted uranium predictably being one of the major and significant nuclear residues. Other representative radionuclides such as ^{99}Tc and ^{137}Cs, which arise as the products of nuclear fission of ^{235}U and ^{239}Pu, also account for a large proportion of nuclear waste streams. In addition, Sr^{II}, Th^{IV}, and radiological iodine are also pervasive in the waste from nuclear reactions. To ensure the safe disposal of radioactive waste, significant progress has been made, and a variety of separation technologies have been developed to sequestrate radioactive materials from legacy waste. However, concerns over factors such as low efficiency and ineluctable byproducts still urge

increasing research for the development of improved nuclear wastewater treatment. Recently, an advanced adsorption technology based on APMs has been generally accepted as a promising application for the elimination of radionuclides with high efficiency and low cost.

Amidoxime (–C(NOH)NH_2, AO) has been widely recognized as the premier chelator for binding uranium.[83] Because of this, diverse APMs have been designed as decorating platforms to anchor AO groups in various forms to enhance their performance in the selective extraction of uranium. Ma et al. conducted a series of in-depth studies of decorating COPs with AO moieties and their applicability for capturing uranium in a variety of systems. PAF-1 was first chosen by Ma and co-workers as the ideal platform for exploiting advanced adsorbents in the sequestration of uranium.[84] To do this, PAF-1 was decorated by AO moieties through a three-step post-synthetic modification. After the chloromethylation of PAF-1 was complete, NaCN was added to replace –Cl with –CN and followed by treatment with hydroxylamine to transform the cyano group into amidoxime, yielding PAF-1-CH_2AO.[84a] The saturated uranium uptake capacity of the resulting adsorbent material was estimated to be 304 mg g^{-1} and PAF-1-CH_2AO showed a rapid removal efficiency from aqueous solution (from 4100 ppb to 0.81 ppb in 90 min.) (Table S3). Given that amidoxime typically binds to uranyl ions in an η^2 coordination manner, the rational modification of open-chain amidoxime moieties would lead to enhanced binding and consequent uptake. Based on this assumption, we grafted amidoxime chains with different lengths on PAF-1 to afford two new adsorbent materials, PAF-1-CH_2NHAO and PAF-1-NH$(CH_2)_2$AO.[84b] The sorption results revealed that the uranium uptake of PAF-1-NH$(CH_2)_2$AO was nearly 4-fold higher than that of PAF-1-CH_2NHAO, which can be attributed to improved binding in PAF-1-NH$(CH_2)_2$AO due to the increased flexibility of AO moieties. What's more, the binding activity of the same chelators can also be precisely tuned by placing secondary-sphere modifiers in a suitable position, manipulating their spatial distribution in networks, and modifying the distances and angles of chelators at the molecular level. Accordingly, Ma and co-workers presented three types of novel POP-based adsorbents to conduct this proof-of-concept study. The optimized adsorbent materials, POP-$o$$NH_2$-AO,[85] POP2-$PO_3H_2$,[86] and POP_1-AO,[87] all exhibited extremely high affinity toward uranium and excellent recovery of uranium from natural seawater (4.36, 5.01, and 8.40 mg g^{-1} for POP-$o$$NH_2$-AO, POP2-$PO_3H_2$, and POP_1-AO, respectively) (Figure 15). In addition to this, all POP-based adsorbents lowered the level of uranium in aqueous solution from a ppm level to less than 1 ppb, disclosing their promising application in the purification of nuclear wastewater containing uranium.

While the incremental density and flexibility of chelators found in amorphous POPs have proven extremely useful, the ordered arrangement of chelators in adsorbents has shown promise as an alternative strategy for improving the accessibility as well as the cooperation between chelators leading to improved binding affinity. 2D COFs with unique structures offer us a great research platform to fulfill this

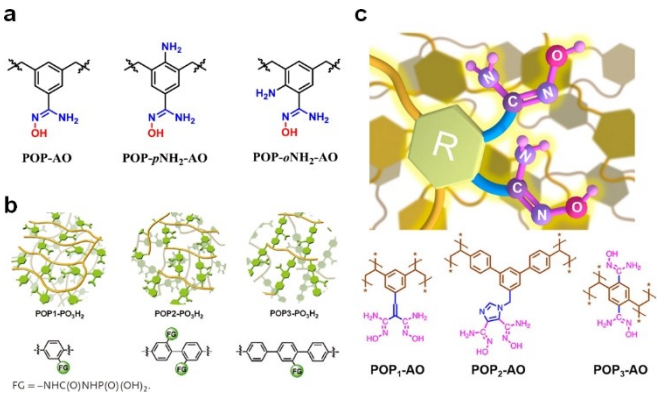

Figure 15. a) Building units of various amidoxime-functionalized hierarchical porous polymers. Reproduced with permission.[85] Copyright 2018, Springer Nature. b) Cartoon structures of various phosphorylurea-functionalized hierarchical porous polymers. Reproduced with permission.[86] Copyright 2020, Wiley-VCH. c) Porous frameworks constructed by uranyl-specific ligand "hooks" and the corresponding structures of diamidoxime-functionalized POPs. Reproduced with permission.[87] Copyright 2021, American Chemical Society.

task. The COF-TpDb-AO obtained by the condensation of TFP with 2,5-diaminobenzonitrile followed by the amidoximation was presented by Ma and co-workers for removing uranium from various uranium-contaminated water samples (Figure 16).[88] A uranium uptake capacity of 408 mg g^{-1} was

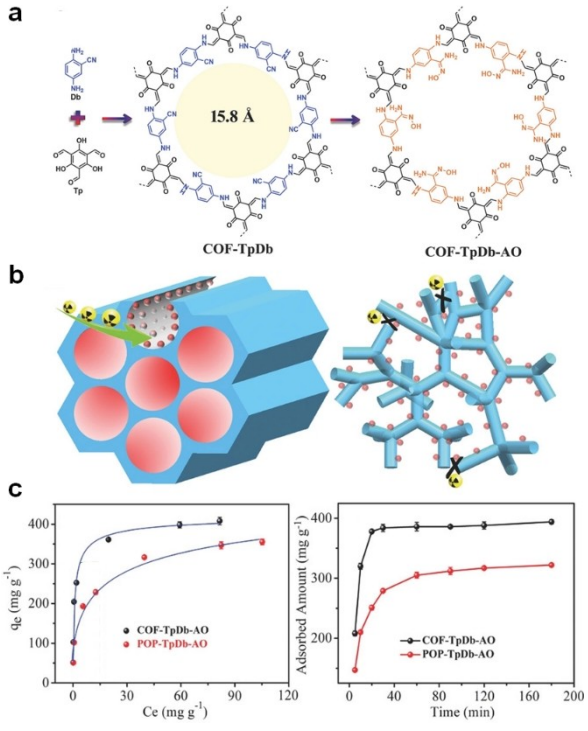

Figure 16. a) Synthesis of COF-TpDb and corresponding chemical transformation of the cyano to amidoxime group, yielding COF-TpDb-AO. b) Schematic illustration of chelating groups in COF and POP materials. c) Comparison of uranium sorption for COF- and POP-based sorbents. Reproduced with permission.[88] Copyright 2018, Wiley-VCH.

estimated for COF-TpDb-AO, while the corresponding amorphous analog (POP-TpDb-AO) demonstrated a lower value of 355 mg g^{-1}. Additionally, COF-TpDb-AO had a more rapid absorption rate and was able to reach 95 % of its maximum adsorption capacity within 0.5 h; triple that time was required for its amorphous analog to yield a comparable value. A higher binding affinity toward uranium was also found in COF-TpDb-AO as the result of the coincident orientation of its chelators. These merits allowed for COF-TpDb-AO to segregate uranium species from various nuclear wastewater samples, lowering the uranium concentration from 5 ppm to lower than 0.1 ppb within a short time, surpassing the EPA limit of 30 ppb in drinking water by two orders of magnitude. This strategy of generating AO-COFs through amidoximation has also been employed in preparing sp^2 carbon COFs. Qiu and co-workers developed a series of sp^2 carbon COFs.[89] The corresponding AO-COFs were obtained by treating the parent COFs with hydroxylamine to transform the cyano group left by the condensation of acetonitrile monomers into amidoxime. The resulting sp^2 carbon COF adsorbents with AO groups not only feature a strong affinity but also present a conjugated structure that can be tuned as a selective photocatalyst for uranium reduction, thus enhancing its uptake capacity.[89c]

In an attempt to extend the applicability of sorption applications, Zhu and co-workers presented the manipulation to improve the accessibility and affinity of binding sites in a collection of PAFs and, consequently, uranium sequestration performance.[90] To do this, they developed a series of molecularly imprinted porous aromatic frameworks (MIPAFs) using the presynthesized UO_2^{2+}-imprinted complexes (Figure 17).[90a] The resulting MIPAFs showed high

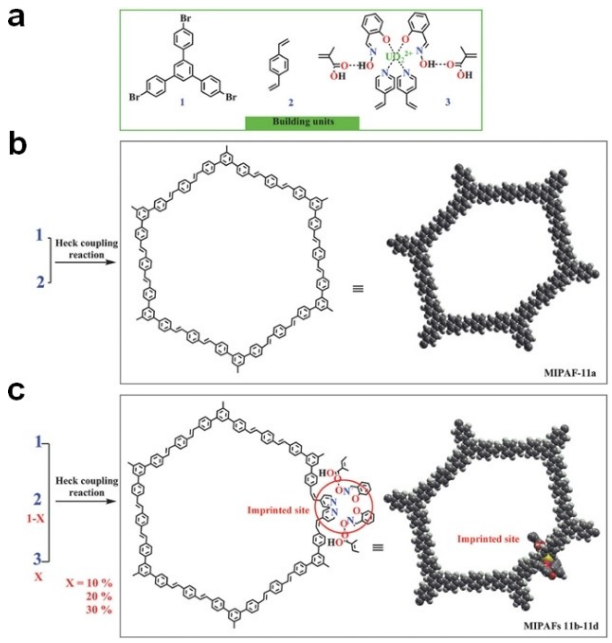

Figure 17. a) Components for the Heck coupling reaction. b) Synthesis and possible fragments for MIPAF-11-a. c) MIPAFs 11b–11d with different pore size distributions what is circled in red to guide the eye. Reproduced with permission.[90a] Copyright 2018, Wiley-VCH.

selectivity toward UO_2^{2+} ion capture in the presence of various competing metal ions. This was attributed to the rigid spatial structure of the imprinted sites in MIPAFs which selectively allowed for the special coordination of the UO_2^{2+} ion. The experimental results revealed that MIPAF-11c had the highest selectivity compared to other benchmark adsorbents at that time, suggesting its potential for uranium recovery from a complex environment such as seawater. Additionally, the concentration of the uranium solution could be reduced from 5 ppm to 0.43 ppb after treatment with MIPAF-11c for 120 min., thus revealing its functionality for water purification.

MOFs, with their outstanding catalytic performance, are also capable of reducing and immobilizing uranium species to improve extraction uptake.[91] Zhang et al. introduced a novel type of MOF constructed by polyoxometalates (POMs) and employed the obtained POM-based MOF, SCU-19, for the sorption of uranium.[91a] The benefits of this material include its strong interaction with U^{VI}, rich redox sites, and photocatalytic activity. In addition to these, the MOF demonstrated excellent performance in uranium uptake and elimination with its highest uptake estimated to be 728.34 mg g^{-1} when the sorption system was irradiated with visible light and showing over 99 % elimination of uranium from a solution with an initial concentration of $\approx$10 ppm in the span of 2 hours.

Apart from unreacted uranium in nuclear residues, technetium-99 produced in a typical reactor can also be found in a large portion of nuclear fission products (841 g ton^{-1}). TcO_4^- is the prime species observed in waste streams and is believed to be one of the most hazardous radiation-derived contaminants due to its extremely long half-life ($t_{1/2} = 2.13 \times 10^5$ years). Separating TcO_4^- at the first stage (when the used fuel is dissolved in nitric acid) before the plutonium–uranium redox extraction process (PUREX) is beneficial for the subsequent treatment of nuclear waste (TcO_4^- will contaminate the extract in PUREX processes). Given the superacidity and high radioactivity of TcO_4^-, the process of its removal by adsorbent materials requires high resistance to both acids and radiation, and high TcO_4^- uptake capacity with excellent selectivity and kinetics. Ion-exchange technology is currently viewed as the most promising method for segregating TcO_4^- from nuclear waste solutions containing a high concentration of various acid anions (e.g., Cl^-, NO_3, SO_4^{2-}) owing to the larger molecule size of TcO_4^- and its lower hydration energy which allow it to be preferentially exchanged over interfering anions.

To stress the utility of POPs for technetium segregation via ion exchange, Ma and co-workers grafted trimethylammonium hydroxide groups onto PAF-1 to afford PAF-1-$CH_2N^+(CH_3)_3OH^-$.[92] The ion-exchange adsorbent produced showed outstanding uptake capacity and kinetics toward MnO_4^-, a common model ion for the assessment of TcO_4^- removal, surpassing some commercially available products including Amberlyst-A26, layered double hydroxides (LDHs), PVBTAH-ZIF-8, and SLUG-21 under the identical conditions.[92a] Following this, Ma and co-workers conducted a study manipulating the binding affinity of the ion-exchange site toward TcO_4^- to improve the performance

of POPs for TcO_4^- remediation. A variety of secondary-sphere modifiers with different distributions of charge density around the aromatic ring were selected and introduced to the *para* position of the pyridinium unit in the resulting POPs to adjust the local environment of the cation site, allowing the ion-exchange performance to be manipulated, and PQA-*p*N(Me)$_2$Py-Cl showcased the highest uptakes of ReO_4^- (a common nonradioactive surrogate for TcO_4^-) among all three PQAs as 1127 mg g^{-1} (also one of the highest uptakes of ReO_4^- thus far, see Table S4) (Figure 18),[93] which was inconsistent with the density of ion-exchange sites in these three adsorbents. Further DFT calculation confirmed that the cationic polymer backbone of PQA-*p*N(Me)$_2$Py-Cl has higher electrostatic ion-pairing attraction energies toward ReO_4^- ions, thus increasing the capacity. Remarkably, the investigation of TcO_4^- removal was performed on real radioactive TcO_4^- water samples. The elimination efficiency of TcO_4^- using the optimized POP, PQA-*p*N(Me)$_2$Py-Cl, was first evaluated in the stimulated Hanford low activity waste (LAW) melter recycle stream, where the concentrations of concomitant acid anions (e.g., NO_3^-, NO_2^-, and Cl^-) were more than 300 times that of TcO_4^-. The results demonstrated that about 95 % of TcO_4^- could be removed from the nuclear wastewater at a phase ratio of 200 mL g^{-1}, even though the huge challenge remained to selectively remove TcO_4^- in the presence of a large number of competing anions. To further investigate the material's effectiveness, the decontamination of TcO_4^- in Savannah River Sites was also tested. From this, it was observed that approximately 80 % of TcO_4^- could be separated from the basic water samples in the presence of a high concentration of other anions with a combined strength of over 70 000 times that of TcO_4^- at a phase ratio of 100 mL g^{-1}. This reported value shows the great potential of the synthesized POPs, as they outperformed all reported materials at the time.

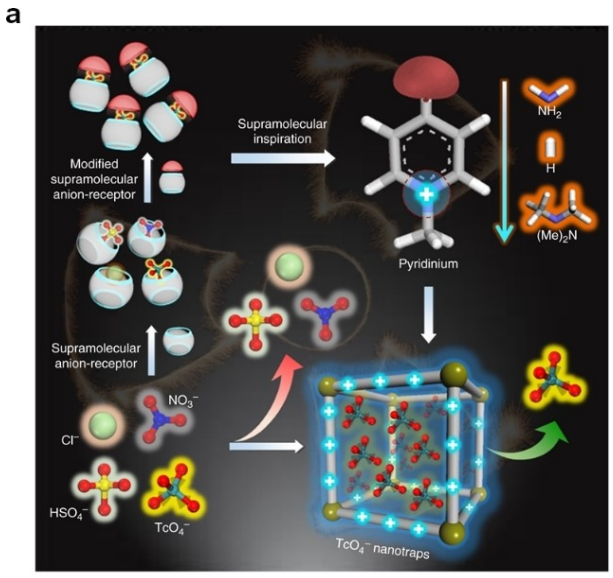

PQA	BET surface area ($m^2 g^{-1}$)	Pore volume ($cm^3 g^{-1}$)
PQA-Py-I	465	0.645
PQA-*p*NH$_2$Py-I	344	0.238
PQA-*p*N(Me)$_2$Py-I	223	0.15

Figure 18. a) Anion nanotraps for TcO_4^- removal. Illustration of optimizing pyridinium-based anion nanotraps for TcO_4^- recognition inspired by supramolecular technology. b) Structure of building units and textural parameters of various pyridinium-functionalized hierarchical porous polymers. Reproduced with permission.[93] Copyright 2019, Springer Nature.

Wang and co-workers reported several cationic polymeric networks (SCU-CPN-X) that demonstrated remarkable sorption kinetics and uptake capacity for TcO_4^-.[94] One of the resulting frameworks, SCU-CPN-1 (Figure 19),[94a] showed outstanding hydrolytic stability in strong acid solutions as well as exceptional resistance toward high-energy ionizing radiation (e.g., β-rays and γ-rays). The group also reported the application of radiation-resistant crystalline polymers in the selective trapping of TcO_4^-.[95] The cationic MOF material (SCU-101) with abundant open Ag^+ sites has shown the capacity to efficiently and selectively encapsulate TcO_4^- through a structural transformation process. The potential use of SCU-101 for the removal of TcO_4^- and treatment of nuclear waste was investigated using the stimulated Hanford LAW melter recycle stream. The results from this experiment showed a removal efficiency of 75.2 % for TcO_4^- at a phase ratio of 100 mL g^{-1}. Following this, the group also presented the first example of using a COF-based cationic adsorbent (SCU-COF-1) for TcO_4^- removal under extreme conditions.[96] This 2D cationic COF was synthesized from the condensation of aminated viologen and TFP. The occurrence of tautomerization from the enol form to the keto form in the resulting COF can drastically enhance the stability of the adsorbent material. After 14 h of adsorption in the simulated Hanford LAW melter recycle stream using SCU-COF-1, 62.8 % removal of TcO_4^- was reported at a solid/liquid ratio of 5, showcasing the applicability of cationic COF materials as ion-exchange adsorbents for the sequestration of anionic pollutants from nuclear wastewater. Very recently, Wang and co-workers reported another successful application of COFs which could be used to recognize and separate palladium in harsh conditions, realizing the efficient recovery of noble metals from used nuclear fuel.[97]

The presence of radioactive iodine in nuclear fission products and natural gas production represents severe environmental and health hazards because of its mode of β-decay. In an effort to efficiently remove the iodine from aqueous solution, several judicious binding site designs have recently been developed utilizing a series of N heteroatomic units (e.g., amine, imine, pyrrole, and various N-containing rings) grafted onto the porous adsorbents for enhanced iodine sorption. The binding affinity toward iodine can also be improved by a π-conjugated structure. Based on these facts, a family of triazine-based CMPs (TCMPs) was

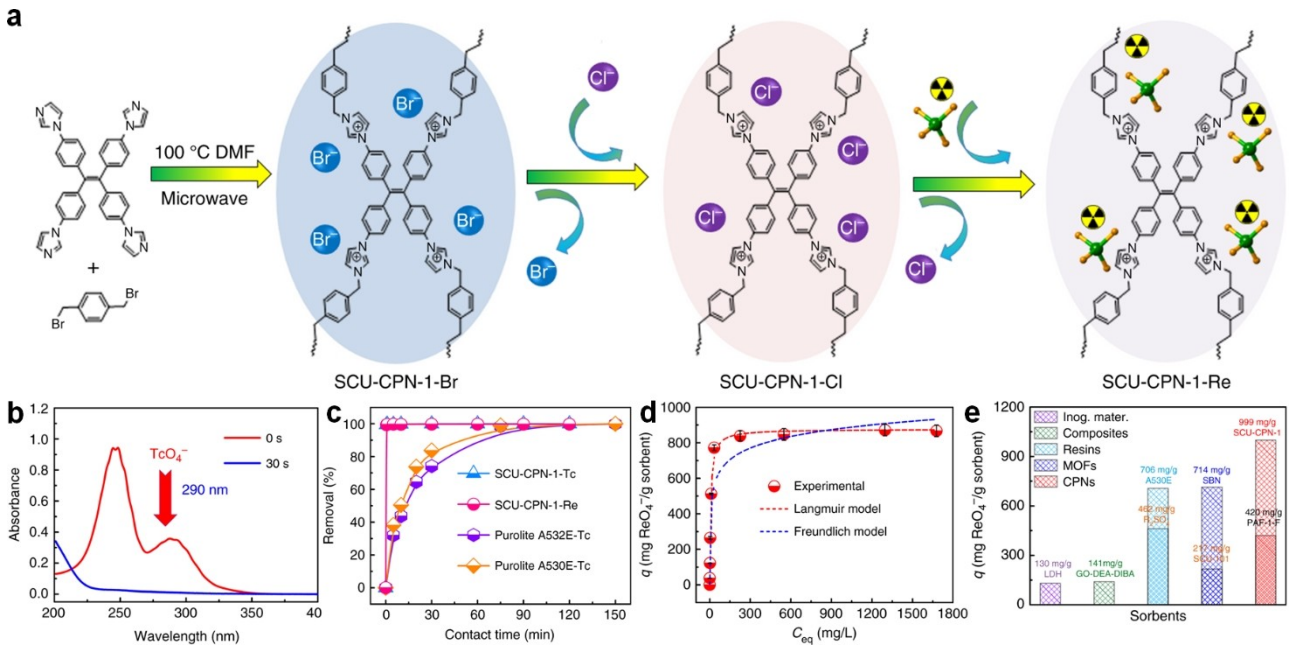

Figure 19. a) Synthesis of SCU-CPN-1 and its anion-exchange applications. b) UV/Vis spectra of TcO_4^- solution during the anion-exchange with SCU-CPN-1. c) Kinetics for the sorption of TcO_4^- by SCU-CPN-1 compared with Purolite A530E and Purolite A532E. d) Sorption isotherm of SCU-CPN-1 for ReO_4^- uptake. e) ReO_4^- sorption capacity of SCU-CPN-1 compared with other reported anion sorbents. Error bars represent standard deviation of three independent experiments. Reproduced with permission.[94a] Copyright 2018, Springer Nature.

synthesized and investigated for their effectiveness in I_2 removal in both the gas phase and in solution.[98] By combining the merits of the N-containing group (triazine) and π-conjugated network, three amorphous TCMPs were constructed via a Friedel–Crafts polymerization of 2,4,6-trichloro-1,3,5-triazine (TCT) and three triphenylamine derivatives. All materials demonstrated excellent adsorption capacity of I_2 vapor (4.90, 3.13, and 3.04 $g\,g^{-1}$ for TPPA, TTDAB, and Tm-MTDAB, respectively), as well as efficient removal of I_2 from solution (higher than 80% for all TCMPs). This performance was attributed to the abundance of sorption sites, twisted propeller-like conformation, and charge-transfer interactions. Moreover, the ordered 1D channels in porous materials played a supporting role, allowing for accessibility and cooperation between binding sites as discussed above. Wang et al. reported a library of 2D COFs with uniform 1D open channels for I_2 capture accordingly.[99] The highest adsorption capacity of I_2 vapor (6.26 $g\,g^{-1}$) among all 2D COFs studied in this report was achieved using TPB-DMTP COF. Additionally, the spent TPB-DMTP COFs can be regenerated by a simple rinse of methanol and retained over 97% pore accessibility as well as the original crystallinity and porosity after five cycles, which thus indicates the material's high chemical/thermal stability in the I_2 adsorption/desorption processes.

To further improve the I_2 sorption performance in POPs, Zhu and co-workers presented a series of PAFs (PAF-23, PAF-24, and PAF-25) containing anionic borate sites that were synthesized via a Sonogashira–Hagihara coupling reaction of a tetrahedral building unit (lithium tetrakis(4-iodophenyl)-borate) and diverse alkyne monomers (Figure 20).[100] The PAFs bearing three effective sorption sites,

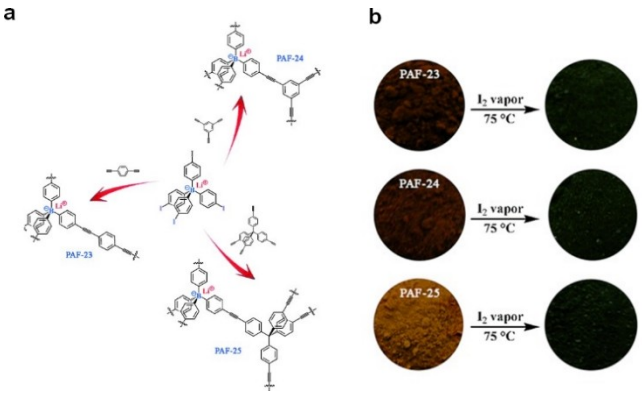

Figure 20. a) Synthesis of polymers PAF-23, PAF-24, and PAF-25 by a Sonogashira–Hagihara coupling reaction. b) Photographs showing the color change before and after iodine capture for polymer networks PAF-23, PAF-24, and PAF-25. Reproduced with permission.[100] Copyright 2015, Wiley-VCH.

which included an ionic site, phenyl rings, and triple bonds, exhibited an excellent affinity for iodine. From these, a high iodine adsorption capability was observed: 2.71, 2.76, and 2.60 $g\,g^{-1}$ for PAF-23, PAF-24, and PAF-25, respectively, at 348 K. What's more, the iodine sorption of PAFs was further evaluated using an I_2 solution and after 24 h of contact, an obvious discoloration of the I_2 solution could be observed upon the addition of PAF-24, which outperformed other types of adsorbents (e.g., Zeolite 13X and CMP E1) under the same conditions.

4. Conclusions and Perspectives

The combination of well-defined pore structures and tailored functionality in advanced porous materials endows them with significant potential for the decontamination of a variety of pollutants present in water supplies. As one of the most pressing environmental issues, the efficient elimination of hazardous contaminants and purification of surface water is directly responsible for the prosperity and the welfare of our global ecosystem as well as each individual human. Families of novel porous materials, including MOFs, COFs, and POPs, are performing significant roles in this respect due to their unparalleled merits in sorption applications such as rapid sorption kinetics, high uptake capacity, and exceptional selectivity. In this Review, we present the recent advances in the use of APM-based adsorbent materials for the segregation of pollutants in water. Despite substantial gains that have recently been made in the research of APMs, an expanse of untapped potential remains, which will continue to increase the effectiveness of related materials as these areas are unveiled by future studies. To fully explore this promising potential in the areas of environmental remediation and water purification, we would like to provide some recommendations to address the present challenges which are hindering their real-world applications.

One major challenge involving the applicability of functional APMs is the difficulty in the preparation and processing of bulk material. Because of this, more effective synthesis methods are required to increase the yield. As of today, the production of APMs is typically energy demanding and accompanied by a large amount of greenhouse gas emissions. In addition, these task-specific APM-based adsorbents are often prepared by cumbersome synthetic procedures, further impeding their use in practical applications. To address this issue, future research should be directed in an effort to develop affordable APMs from environment-friendly and inexpensive raw materials and with improved synthesis methods. From this, the large-scale sustainable manufacturing of APM-based materials is crucially necessary to meet industrial needs and can ensure the success of using these novel materials outside of the lab. Another hurdle for implementing APMs in earnest is registration, such as U.S. EPA and EU REACH registration, which might be associated with particularly drinking water applications. Usually, for registration of a potential product, its chemical composition, usage, risks, and public benefits will be carefully evaluated, to ensure the product will not cause unreasonable negative effects on the environment or humans. Only after being verified and registered by professional organizations can APMs be launched on the market; otherwise, the public will not have enough confidence in using those materials for drinking water purification. Unfortunately, only a very few APMs have been registered and are available on the market nowadays. What's more, the registration requirements usually vary in different countries, thus resulting in added difficulty in promoting APMs for practical applications. The third goal among future work should be the development of novel adsorbents based on the molecular-level understanding extending to the macroscopic scale. Although it is indispensable to study the direct interactions between adsorbates and binding sites to optimize the performance of adsorbents, the trade-off between surface area and active functional groups always exists and may hinder the transportation of guest species. Thus, an in-depth investigation of the relationship between sorption performance and macroscopic forms is highly necessary and may help to minimize the adverse impacts of APM assembly. Finally, the implementation of APMs in actual water bodies for water purification is much more difficult than in the lab setting because of the harsh conditions and the complex mixture of multiple interfering components present. Therefore, research focusing on enhancing the chemical/hydrolytic stability and selective adsorption of APMs is of great significance and should be conducted.

The world has witnessed significant progress in the application of APMs in the past decades due to their unparalleled versatility. However, the challenges in efficient environmental remediation in real-world settings remain. We believe that such problems can be properly addressed in the foreseeable future with the rapid development of technology and the impending development of large-scale applications of APMs for water purification approaches.

Acknowledgements

The authors acknowledge the Robert A. Welch Foundation (B-0027), the United States National Science Foundation (CBET-1706025), and the DOE Office of Nuclear Energy's Nuclear Energy University Program (Grant DE-NE0008281) for support of this work.

Conflict of Interest

The authors declare no conflict of interest.

Keywords: Covalent Organic Frameworks · Metal-Organic Frameworks · Porous Organic Polymers · Task-Specific Design · Water Purification

[1] a) K. Bakker, *Science* **2012**, *337*, 914–915; b) C. J. Vörösmarty, P. B. McIntyre, M. O. Gessner, D. Dudgeon, A. Prusevich, P. Green, S. Glidden, S. E. Bunn, C. A. Sullivan, C. Reidy Liermann, P. M. Davies, *Nature* **2010**, *467*, 555–561; c) M. Haseena, M. F. Malik, A. Javed, S. Arshad, N. Asif, S. Zulfiqar, J. Hanif, *Environ. Risk Assess. Remediat.* **2017**, *1*, 3.

[2] a) M. Petrovic, S. Gonzalez, D. Barcelo, *Trends Analyt. Chem.* **2003**, *22*, 685–696; b) N. Bolong, A. F. Ismail, M. R. Salim, T. Matsuura, *Desalination* **2009**, *239*, 229–246; c) H. Abu Hasan, M. H. Muhammad, N. I. Ismail, *J. Water Proc. Eng.* **2020**, *33*, 101035; d) A. Mirzaei, Z. Chen, F. Haghighat, L. Yerushalmi, *Chemosphere* **2017**, *174*, 665–688.

[3] a) M. A. Shannon, P. W. Bohn, M. Elimelech, J. G. Georgiadis, B. J. Marinas, A. M. Mayes, *Nature* **2008**, *452*, 301–310; b) S. Bolisetty, M. Peydayesh, R. Mezzenga, *Chem. Soc. Rev.*

2019, *48*, 463–487; c) A. Lee, J. W. Elam, S. B. Darling, *Environ. Sci.: Water Res. Technol.* **2016**, *2*, 17–42; d) D. Deng, W. Aouad, W. A. Braff, S. Schlumpberger, M. E. Suss, M. Z. Bazant, *Desalination* **2015**, *357*, 77–83; e) A. Bhatnagar, M. Sillanpaa, A. Witek-Krowiak, *Chem. Eng. J.* **2015**, *270*, 244–271.

[4] a) R. Andreozzi, V. Caprio, A. Insola, R. Marotta, *Catal. Today* **1999**, *53*, 51–59; b) H. Choi, S. R. Al-Abed, D. D. Dionysiou, E. Stathatos, P. Lianos, *Sustain. Sci. Eng.* **2010**, *2*, 229–254; c) B. Huang, Z. Wu, H. Zhou, J. Li, C. Zhou, Z. Xiong, Z. Pan, G. Yao, B. Lai, *J. Hazard. Mater.* **2021**, *412*, 125253; d) S. Licht, X. Yu, *Environ. Sci. Technol.* **2005**, *39*, 8071–8076; e) D. Li, J. Qu, *J. Environ. Sci.* **2009**, *21*, 713–719; f) W. C. Ellis, C. T. Tran, R. Roy, M. Rusten, A. Fischer, A. D. Ryabov, B. Blumberg, T. J. Collins, *J. Am. Chem. Soc.* **2010**, *132*, 9774–9781; g) G. Yu, Y. Wang, H. Cao, H. Zhao, Y. Xie, *Environ. Sci. Technol.* **2020**, *54*, 5931–5946; h) D.-N. Pei, C. Liu, A.-Y. Zhang, X.-Q. Pan, H.-Q. Yu, *Proc. Natl. Acad. Sci. USA* **2020**, *117*, 30966–30972; i) A. M. Karpinska, J. Bridgeman, *Water Res.* **2016**, *88*, 861–879; j) A. Moura, M. Tacão, I. Henriques, J. Dias, P. Ferreira, A. Correia, *Microbiol. Res.* **2009**, *164*, 560–569; k) T. Bressani-Ribeiro, P. G. S. Almeida, E. I. P. Volcke, C. A. L. Chernicharo, *Environ. Sci.: Water Res. Technol.* **2018**, *4*, 1721–1738; l) F. Hassard, J. Biddle, E. Cartmell, B. Jefferson, S. Tyrrel, T. Stephenson, *Process Saf. Environ. Prot.* **2015**, *94*, 285–306.

[5] a) S. Chowdhury, M. A. J. Mazumder, O. Al-Attas, T. Husain, *Sci. Total Environ.* **2016**, *569–570*, 476–488; b) L. Joseph, B.-M. Jun, J. R. V. Flora, C. M. Park, Y. Yoon, *Chemosphere* **2019**, *229*, 142–159; c) M. Bilal, I. Ihsanullah, M. Younas, M. U. H. Shah, *Sep. Purif. Technol.* **2021**, *278*, 119510.

[6] a) Z. Liu, K. Demeestere, S. V. Hulle, *J. Environ. Chem. Eng.* **2021**, *9*, 105599; b) J. T. Alexander, F. I. Hai, T. M. Al-aboud, *J. Environ. Manage.* **2012**, *111*, 195–207; c) Z.-M. Song, Y.-L. Xu, J.-K. Liang, L. Peng, X.-Y. Zhang, Y. Du, Y. Lu, X.-Z. Li, Q.-Y. Wu, Y.-T. Guan, *Water Res.* **2021**, *190*, 116733; d) M. J. Capdeville, H. Budzinski, *TrAC Trends Anal. Chem.* **2011**, *30*, 586–606; e) J. C. G. Sousa, A. R. Ribeiro, M. O. Barbosa, M. F. R. Pereira, A. M. T. Silva, *J. Hazard. Mater.* **2018**, *344*, 146–162.

[7] a) B. Pan, B. Xing, *Environ. Sci. Technol.* **2008**, *42*, 9005–9013; b) I. Ali, *Chem. Rev.* **2012**, *112*, 5073–5091; c) M. K. Uddin, *Chem. Eng. J.* **2017**, *308*, 438–462; d) C. Sophia A, E. C. Lima, *Ecotoxicol. Environ. Saf.* **2018**, *150*, 1–17; e) I. Ali, *Sep. Purif. Rev.* **2014**, *43*, 175–205; f) M. T. Yagub, T. K. Sen, S. Afroze, H. M. Ang, *Adv. Colloid Interface Sci.* **2014**, *209*, 172–184; g) G. Alam, I. Ihsanullah, M. Naushad, M. Sillanpaa, *Chem. Eng. J.* **2022**, *427*, 130011; h) M. J. Ahmed, B. H. Hameed, E. H. Hummadi, *Carbohydr. Polym.* **2020**, *247*, 116690.

[8] a) A. G. Slater, A. I. Cooper, *Science* **2015**, *348*, aaa8075; b) Q. Sun, B. Aguila, Y. Song, S. Ma, *Acc. Chem. Res.* **2020**, *53*, 812–821; c) J. H. Pan, H. Dou, Z. Xiong, C. Xu, J. Ma, X. S. Zhao, *J. Mater. Chem.* **2010**, *20*, 4512–4528; d) L. Zhu, D. Shen, K. H. Luo, *J. Hazard. Mater.* **2020**, *389*, 122102.

[9] a) A. Bhatnagar, W. Hogland, M. Marques, M. Sillanpaa, *Chem. Eng. J.* **2013**, *219*, 499–511; b) W. Tian, H. Zhang, X. Duan, H. Sun, G. Shao, S. Wang, *Adv. Funct. Mater.* **2020**, *30*, 1909265.

[10] a) N. Jiang, R. Shang, S. G. J. Heijman, L. C. Rietveld, *Water Res.* **2018**, *144*, 145–161; b) S. Wang, Y. Peng, *Chem. Eng. J.* **2010**, *156*, 11–24.

[11] a) P. N. E. Diagboya, E. D. Dikio, *Microporous Mesoporous Mater.* **2018**, *266*, 252–267; b) E. Da′na, *Microporous Mesoporous Mater.* **2017**, *247*, 145–157.

[12] a) R. J. Drout, L. Robison, Z. Chen, T. Islamoglu, O. K. Farha, *Trends Chem.* **2019**, *1*, 304–317; b) J. Li, H. Wang, X. Yuan, J. Zhang, J. W. Chew, *Coord. Chem. Rev.* **2020**, *404*, 213116; c) Q. Gao, J. Xu, X.-H. Bu, *Coord. Chem. Rev.* **2019**, *378*, 17–31; d) H. Gul Zaman, L. Baloo, R. Pendyala, P. K. Singa, S. U. Ilyas, S. R. M. Kutty, *Materials* **2021**, *14*, 7607; e) Y. Li, M. Kairmi, Y.-N. Gong, N. Dai, V. Safarifard, H.-L. Jiang, *Matter* **2021**, *4*, 2230–2265; f) F. Yang, M. Du, K. Yin, Z. Qiu, J. Zhao, C. Liu, G. Zhang, Y. Gao, H. Pang, *Small* **2022**, *18*, 2105715; g) Y. Yao, C. Wang, J. Na, M. S. A. Hossain, X. Yan, H. Zhang, M. A. Amin, J. Qi, Y. Yamauchi, J. Li, *Small* **2022**, *18*, 2104387.

[13] a) J. Chakraborty, I. Nath, F. Verpoort, *Chem. Soc. Rev.* **2022**, *51*, 1124–1138; b) L. Huang, R. Liu, J. Yang, Q. Shuai, B. Yuliarto, Y. V. Kaneti, Y. Yamauchi, *Chem. Eng. J.* **2021**, *408*, 127991; c) B. Zheng, X. Lin, X. Zhang, D. Wu, K. Matyjaszewski, *Adv. Funct. Mater.* **2020**, *30*, 1907006; d) J. Wu, F. Xu, S. Li, P. Ma, X. Zhang, Q. Liu, R. Fu, D. Wu, *Adv. Mater.* **2019**, *31*, 1902922; e) D. Taylor, S. J. Dalgarno, Z. Xu, F. Vilela, *Chem. Soc. Rev.* **2020**, *49*, 3981–4042; f) M. G. Mohamed, A. F. M. EL-Mahdy, M. G. Kotp, S.-W. Kuo, *Mater. Adv.* **2022**, *3*, 707–733.

[14] a) Z. Xia, Y. Zhao, S. B. Darling, *Adv. Mater. Interfaces* **2021**, *8*, 2001507; b) J. Wang, S. Zhuang, *Coord. Chem. Rev.* **2019**, *400*, 213046; c) X. Liu, H. Pang, X. Liu, Q. Li, N. Zhang, L. Mao, M. Qiu, B. Hu, H. Yang, X. Wang, *Innovation* **2021**, *2*, 100076; d) I. Ahmed, S. H. Jhung, *Coord. Chem. Rev.* **2021**, *441*, 213989; e) A. R. Bagheri, N. Aramesh, Z. Liu, C. Chen, W. Shen, S. Tang, *Crit. Rev. Anal. Chem.* **2022**, https://doi.org/10.1080/10408347.2022.2089838; f) A. K. Mohammed, D. Shetty, *Environ. Sci.: Water Res. Technol.* **2021**, *7*, 1895–1927.

[15] a) H.-C. Zhou, S. Kitagawa, *Chem. Soc. Rev.* **2014**, *43*, 5415–5418; b) H.-C. Zhou, J. R. Long, O. M. Yaghi, *Chem. Rev.* **2012**, *112*, 673–674; c) H. Furukawa, K. E. Cordova, M. O'Keeffe, O. M. Yaghi, *Science* **2013**, *341*, 1230444; d) S. Yuan, L. Feng, K. Wang, J. Pang, M. Bosch, C. Lollar, Y. Sun, J. Qin, X. Yang, P. Zhang, Q. Wang, L. Zou, Y. Zhang, L. Zhang, Y. Fang, J. Li, H.-C. Zhou, *Adv. Mater.* **2018**, *30*, 1704303.

[16] a) S.-Y. Ding, W. Wang, *Chem. Soc. Rev.* **2013**, *42*, 548–568; b) Y. Song, Q. Sun, B. Aguila, S. Ma, *Adv. Sci.* **2019**, *6*, 1801410; c) N. Huang, P. Wang, D. Jiang, *Nat. Rev. Mater.* **2016**, *1*, 16068.

[17] a) Y. Tian, G. Zhu, *Chem. Rev.* **2020**, *120*, 8934–8986; b) J.-S. M. Lee, A. I. Cooper, *Chem. Rev.* **2020**, *120*, 2171–2214; c) D. Wu, F. Xu, B. Sun, R. Fu, H. He, K. Matyjaszewski, *Chem. Rev.* **2012**, *112*, 3959–4015.

[18] a) S. Mandal, S. Natarajan, P. Mani, A. Pankajakshan, *Adv. Funct. Mater.* **2021**, *31*, 2006291; b) J. L. Segura, S. Royuela, M. M. Ramos, *Chem. Soc. Rev.* **2019**, *48*, 3903–3945; c) J. H. Kim, D. W. Kang, H. Yun, M. Kang, N. Singh, J. S. Kim, C. S. Hong, *Chem. Soc. Rev.* **2022**, *51*, 43–56; d) Z. Wang, S. M. Cohen, *Chem. Soc. Rev.* **2009**, *38*, 1315–1329.

[19] a) R.-R. Liang, S.-Y. Jiang, R.-H. A, X. Zhao, *Chem. Soc. Rev.* **2020**, *49*, 3920–3951; b) Y. Jin, Y. Hu, W. Zhang, *Nat. Chem. Rev.* **2017**, *1*, 0056.

[20] V. K. Gupta Suhas, *J. Environ. Manage.* **2009**, *90*, 2313–2342.

[21] a) A. Sridhar, M. Ponnuchamy, A. Kapoor, S. Prabhakar, *J. Hazard. Mater.* **2022**, *424*, 127432; b) L. Bulgariu, L. B. Escudero, O. S. Bello, M. Iqbal, J. Nisar, K. A. Adegoke, F. Alakhras, M. Kornaros, I. Anastopoulos, *J. Mol. Liq.* **2019**, *276*, 728–747.

[22] a) B. Lellis, C. Z. Favaro-Polonio, J. A. Pamphile, J. C. Polonio, *Biotechnol. Res. Innov.* **2019**, *3*, 275–290; b) A. Y. L. Tang, C. K. Y. Lo, C.-W. Kan, *Color. Technol.* **2018**, *134*, 245–

257; c) K.-T. Chung, *J. Environ. Sci. Health Part C* **2016**, *34*, 233–261.
[23] S. Basu, M. Maes, A. Cano-Odena, L. Alaerts, D. E. De Vos, I. F. J. Vankelecom, *J. Membr. Sci.* **2009**, *344*, 190–198.
[24] R. Zhang, S. Ji, N. Wang, L. Wang, G. Zhang, J.-R. Li, *Angew. Chem. Int. Ed.* **2014**, *53*, 9775–9779; *Angew. Chem.* **2014**, *126*, 9933–9937.
[25] M. S. Denny, S. M. Cohen, *Angew. Chem. Int. Ed.* **2015**, *54*, 9029–9032; *Angew. Chem.* **2015**, *127*, 9157–9160.
[26] S. Kandambeth, B. P. Biswal, H. D. Chaudhari, K. C. Rout, S. Kunjattu H, S. Mitra, S. Karak, A. Das, R. Mukherjee, U. K. Kharul, R. Banerjee, *Adv. Mater.* **2017**, *29*, 1603945.
[27] W. Zhang, L. Zhang, H. Zhao, B. Lin, H. Ma, *J. Mater. Chem. A* **2018**, *6*, 13331–13339.
[28] a) T. Düren, Y.-S. Bae, R. Q. Snurr, *Chem. Soc. Rev.* **2009**, *38*, 1237–1247; b) J. Canivet, A. Fateeva, Y. Guo, B. Coasne, D. Farrusseng, *Chem. Soc. Rev.* **2014**, *43*, 5594–5617; c) M. Wen, G. Li, H. Liu, J. Chen, T. An, H. Yamashita, *Environ. Sci. Nano* **2019**, *6*, 1006–1025; d) D. Wu, P.-F. Zhang, G.-P. Yang, L. Hou, W.-Y. Zhang, Y.-F. Han, P. Liu, Y.-Y. Wang, *Coord. Chem. Rev.* **2021**, *434*, 213709; e) C. Petit, *Curr. Opin. Chem. Eng.* **2018**, *20*, 132–142; f) T. Ghanbari, F. Abnisa, W. M. A. W. Daud, *Sci. Total Environ.* **2020**, *707*, 135090.
[29] E. Haque, J. W. Jun, S. H. Jhung, *J. Hazard. Mater.* **2011**, *185*, 507–511.
[30] H. Li, X. Cao, C. Zhang, Q. Yu, Z. Zhao, X. Niu, X. Sun, Y. Liu, L. Ma, Z. Li, *RSC Adv.* **2017**, *7*, 16273–16281.
[31] a) A. A. Al-Gheethi, Q. M. Azhar, P. S. Kumar, A. A. Yusuf, A. K. Al-Buriahi, R. M. S. R. Mohamed, M. M. Al-shaibani, *Chemosphere* **2022**, *287*, 132080; b) A. K. Al-Buriahi, A. A. Al-Gheethi, P. S. Kumar, R. M. S. R. Mohamed, H. Yusof, A. F. Alshalif, N. A. Khalifa, *Chemosphere* **2022**, *287*, 132162.
[32] Y. Li, W. Chen, W. Hao, Y. Li, L. Chen, *ACS Appl. Nano Mater.* **2018**, *1*, 4756–2761.
[33] J. L. Fenton, D. W. Burke, D. Qian, M. O. De la Cruz, W. R. Dichtel, *J. Am. Chem. Soc.* **2021**, *143*, 1466–1473.
[34] a) Y. Liu, Y. Cui, C. Zhang, J. Du, S. Wang, Y. Bai, Z. Liang, X. Song, *Chem. Eur. J.* **2018**, *24*, 7480–7488; b) Y. Wang, Y. Xie, Y. Zhang, S. Tang, C. Guo, J. Wu, R. Lau, *Chem. Eng. Res. Des.* **2016**, *114*, 258–267; c) Y. He, T. Xu, J. Hu, C. Peng, Q. Yang, H. Wang, H. Liu, *RSC Adv.* **2017**, *7*, 30500–30505; d) H. Ou, Q. You, J. Li, G. Liao, H. Xia, D. Wang, *RSC Adv.* **2016**, *6*, 98487–98497; e) L. Huang, M. He, B. Chen, Q. Cheng, B. Hu, *ACS Sustainable Chem. Eng.* **2017**, *5*, 4050–4055; f) Y. Zhang, X. Hong, X.-M. Cao, X.-Q. Huang, B. Hu, S.-Y. Ding, H. Lin, *ACS Appl. Mater. Interfaces* **2021**, *13*, 6359–6366.
[35] X.-S. Wang, J. Liu, J. M. Bonefont, D.-Q. Yuan, P. K. Thallapally, S. Ma, *Chem. Commun.* **2013**, *49*, 1533–1535.
[36] Q. Sun, B. Aguila, J. A. Perman, T. Butts, F.-S. Xiao, S. Ma, *Chem* **2018**, *4*, 1726–1739.
[37] A. Li, H.-X. Sun, D.-Z. Tan, W.-J. Fan, S.-H. Wen, X.-J. Qing, G.-X. Li, S.-Y. Li, W.-Q. Deng, *Energy Environ. Sci.* **2011**, *4*, 2062–2065.
[38] R. Du, N. Zhang, H. Xu, N. Mao, W. Duan, J. Wang, Q. Zhao, Z. Liu, J. Zhang, *Adv. Mater.* **2014**, *26*, 8053–8058.
[39] a) Q. Ma, H. Cheng, A. G. Fane, R. Wang, H. Zhang, *Small* **2016**, *12*, 2186–2202; b) H. Saini, E. Otyepkova, A. Schneemann, R. Zboril, M. Otyepka, R. A. Fischer, K. Jayaramulu, *J. Mater. Chem. A* **2022**, *10*, 2751–2785.
[40] C. Yang, U. Kaipa, Q. Z. Mather, X. Wang, V. Nesterov, A. F. Venero, M. A. Omary, *J. Am. Chem. Soc.* **2011**, *133*, 18094–18097.
[41] K.-Y. A. Lin, H. Yang, C. Petit, F.-K. Hsu, *Chem. Eng. J.* **2014**, *249*, 293–301.
[42] R. Yogapriya, K. R. D. Kasibhatta, *ACS Appl. Nano Mater.* **2020**, *3*, 5816–5825.
[43] S. Gai, R. Fan, J. Zhang, X. Zhou, K. Xing, K. Zhu, W. Jia, W. Sui, P. Wang, Y. Yang, *J. Mater. Chem. A* **2021**, *9*, 3369–3378.
[44] a) A. Tufail, W. E. Price, F. I. Hai, *Chemosphere* **2020**, *260*, 127460; b) S. Spahr, M. Teixdo, D. L. Sedlak, R. G. Luthy, *Environ. Sci.: Water Res. Technol.* **2020**, *6*, 15–44; c) S. Yang, F. I. Hai, L. D. Nghiem, W. E. Price, F. Roddick, M. T. Moreira, S. F. Magram, *Bioresour. Technol.* **2013**, *141*, 97–108.
[45] a) S. Rojas, P. Horcajada, *Chem. Rev.* **2020**, *120*, 8378–8415; b) M. J. Klemes, L. P. Skala, M. Ateia, B. Trang, D. E. Helbling, W. R. Dichtel, *Acc. Chem. Res.* **2020**, *53*, 2314–2324; c) S.-Y. Hu, Y.-N. Sun, Z.-W. Feng, F.-O. Wang, Y.-K. Lv, *Chemosphere* **2022**, *286*, 131646.
[46] a) J. Glüge, M. Scheringer, I. T. Cousins, J. C. DeWitt, G. Goldenman, D. Herzke, R. Lohmann, C. A. Ng, X. Trier, Z. Wang, *Environ. Sci. Process. Impacts* **2020**, *22*, 2345–2373; b) Z. Wang, I. T. Cousins, U. Berger, K. Hungerbuhler, M. Scheringer, *Environ. Int.* **2016**, *89–90*, 235–247.
[47] a) E. M. Sunderland, X. C. Hu, C. Dassuncao, A. K. Tokranov, C. C. Wagner, J. G. Allen, *J. Exposure Sci. Environ. Epidemiol.* **2019**, *29*, 131–147; b) S. E. Fenton, A. Ducatman, A. Boobis, J. C. DeWitt, C. Lau, C. Ng, J. S. Smith, S. M. Roberts, *Environ. Toxicol. Chem.* **2021**, *40*, 606–630; c) A. O. De Silva, J. M. Armitage, T. A. Bruton, C. Dassuncao, W. Heiger-Bernays, X. C. Hu, A. Karrman, B. Kelly, C. Ng, A. Robuk, M. Sun, T. F. Webster, E. M. Sunderland, *Environ. Toxicol. Chem.* **2021**, *40*, 631–657.
[48] a) S. Wacławe, K. Krawczyk, D. Silverstri, V. V. T. Padil, M. Řezanka, M. Černík, M. Jaroniec, *Adv. Colloid Interface Sci.* **2022**, *310*, 102807; b) M. J. Weiss-Errico, *J. Inclusion Phenom. Macrocyclic Chem.* **2019**, *95*, 111–117; c) X. Ji, H. Wang, H. Wang, T. Zhao, Z. A. Page, N. M. Khashab, J. L. Sessler, *Angew. Chem. Int. Ed.* **2020**, *59*, 23402–23412; *Angew. Chem.* **2020**, *132*, 23608–23618.
[49] a) L. Xiao, Y. Ling, A. Alsbaiee, C. Li, D. E. Helbling, W. R. Dichtel, *J. Am. Chem. Soc.* **2017**, *139*, 7689–7692; b) A. Alsbaiee, B. J. Smith, L. Xiao, Y. Ling, D. E. Helbling, W. R. Dichtel, *Nature* **2016**, *529*, 190–194; c) M. J. Klemes, Y. Ling, C. Ching, C. Wu, L. Xiao, D. E. Helbling, W. R. Dichtel, *Angew. Chem. Int. Ed.* **2019**, *58*, 12049–12053; *Angew. Chem.* **2019**, *131*, 12177–12181; d) R. Wang, Z.-W. Lin, M. J. Klemes, M. Ateia, B. Trang, J. Wang, C. Ching, D. E. Helbling, W. R. Dichtel, *ACS Cent. Sci.* **2022**, *8*, 663–669; e) L. Xiao, C. Ching, Y. Ling, M. Nasiri, M. J. Klemes, T. M. Reineke, D. E. Helbling, W. R. Dichtel, *Macromolecules* **2019**, *52*, 3747–3752; f) A. Yang, C. Ching, M. Easler, D. E. Helbling, W. R. Dichtel, *ACS Mater. Lett.* **2020**, *2*, 1240–1245.
[50] R.-Q. Wang, X.-B. Wei, Y.-Q. Feng, *Chem. Eur. J.* **2018**, *24*, 10979–10983.
[51] W. Wang, H. Shao, S. Zhou, D. Zhu, X. Jiang, G. Yu, S. Deng, *ACS Appl. Mater. Interfaces* **2021**, *13*, 48700–48708.
[52] W. Ji, L. Xiao, Y. Ling, C. Ching, M. Matsumoto, R. P. Bisbey, D. E. Helbling, W. R. Dichtel, *J. Am. Chem. Soc.* **2018**, *140*, 12677–12681.
[53] X. Liu, C. Zhu, J. Yin, J. Li, Z. Zhang, J. Li, F. Shui, Z. You, Z. Shi, B. Li, X.-H. Bu, A. Nafady, S. Ma, *Nat. Commun.* **2022**, *13*, 2132.
[54] a) R. Li, S. Alomari, T. Islamoglu, O. K. Farha, S. Fernando, S. M. Thagard, T. M. Holsen, M. Wriedt, *Environ. Sci. Technol.* **2021**, *55*, 15162–15171; b) R. Li, S. Alomari, R. Standon, M. C. Wasson, T. Islamoglu, O. K. Farha, T. M. Holsen, S. M. Thagard, D. J. Trivedi, M. Wriedt, *Chem. Mater.* **2021**, *33*, 3276–3285.

[55] K. Liu, S. Zhang, X. Hu, K. Zhang, A. Roy, G. Yu, *Environ. Sci. Technol.* **2015**, *49*, 8657–8665.

[56] K. Sini, D. Bourgeois, M. Idouhar, M. Carboni, D. Meyer, *Mater. Lett.* **2019**, *250*, 92–95.

[57] Y. Wen, Á. Rentería-Gómez, G. S. Day, M. F. Smith, T.-H. Yan, R. O. K. Ozdemir, O. Gutierrez, V. K. Sharma, X. Ma, H.-C. Zhou, *J. Am. Chem. Soc.* **2022**, *144*, 11840–11850.

[58] a) F. Ahmadijokani, H. Molavi, M. Rezakzemi, S. Tajahmadi, A. Bahi, F. Ko, T. M. Aminabhavi, J.-R. Li, M. Arjmand, *Prog. Mater. Sci.* **2022**, *125*, 100904; b) E. Jin, S. Lee, E. Kang, Y. Kim, W. Choe, *Coord. Chem. Rev.* **2020**, *425*, 213526; c) N. Zhuo, Y. Lan, W. Yang, Z. Yang, X. Li, X. Zhou, Y. Liu, J. Shen, X. Zhang, *Sep. Purif. Technol.* **2017**, *177*, 272–280.

[59] S. Lin, Y. Zhao, Y.-S. Yun, *ACS Appl. Mater. Interfaces* **2018**, *10*, 28076–28085.

[60] S. Zhuang, Y. Liu, J. Wang, *J. Hazard. Mater.* **2020**, *383*, 121126.

[61] L. Wen, L. Liu, X. Wang, M.-L. Wang, J.-M. Lin, R.-S. Zhao, *J. Chromatogr. A* **2020**, *1625*, 461275.

[62] L. Huang, N. Mao, Q. Yan, D. Zhang, Q. Shuai, *ACS Appl. Nano Mater.* **2020**, *3*, 319–326.

[63] L. Hou, C. Shan, Y. Song, S. Chen, L. Wojtas, S. Ma, Q. Sun, L. Zhang, *Angew. Chem. Int. Ed.* **2021**, *60*, 14664–14670; *Angew. Chem.* **2021**, *133*, 14785–14791.

[64] M. Alvaro, E. Carbonell, B. Ferrer, F. X. Llabres i Xamena, H. Garcia, *Chem. Eur. J.* **2007**, *13*, 5106–5112.

[65] A. Gómez-Avilés, M. Penas-Garzon, J. Bedia, D. D. Dionysiou, J. J. Rodriguez, C. Belver, *Appl. Catal. B* **2019**, *253*, 253–262.

[66] Y. Wen, M. Feng, P. Zhang, H.-C. Zhou, V. K. Sharma, X. Ma, *ACS ES&T Engg.* **2021**, *1*, 804–826.

[67] R. Yin, Y. Chen, S. He, W. Li, L. Zeng, W. Guo, M. Zhu, *J. Hazard. Mater.* **2020**, *388*, 121996.

[68] Z. Dong, L. Zhang, J. Gong, Q. Zhao, *Chem. Eng. J.* **2021**, *403*, 126383.

[69] Y. Hou, C.-X. Cui, E. Zhang, J.-C. Wang, Y. Li, Y. Zhang, Y. Zhang, Q. Wang, J. Jiang, *Dalton Trans.* **2019**, *48*, 14989–14995.

[70] Z. Xiao, Y. Zhou, X. Xin, Q. Zhang, L. Zhang, R. Wang, D. Sun, *Macromol. Chem. Phys.* **2016**, *217*, 599–604.

[71] a) M. Hua, S. Zhang, B. Pan, W. Zhang, L. Lv, Q. Zhang, *J. Hazard. Mater.* **2012**, *211–212*, 317–331; b) T. A. Davis, B. Volesky, A. Mucci, *Water Res.* **2003**, *37*, 4311–4330; c) A. Demirbas, *J. Hazard. Mater.* **2008**, *157*, 220–229; d) F. Fu, Q. Wang, *J. Environ. Manage.* **2011**, *92*, 407–418.

[72] B. Li, Y. Zhang, D. Ma, Z. Shi, S. Ma, *Nat. Commun.* **2014**, *5*, 5537.

[73] B. Aguila, Q. Sun, J. A. Perman, L. D. Earl, C. W. Abney, R. Elzein, R. Schlaf, S. Ma, *Adv. Mater.* **2017**, *29*, 1700665.

[74] Q. Sun, B. Aguila, J. Perman, L. D. Earl, C. W. Abney, Y. Cheng, H. Wei, N. Nguyen, L. Wojtas, S. Ma, *J. Am. Chem. Soc.* **2017**, *139*, 2786–2793.

[75] S.-Y. Ding, M. Dong, Y.-W. Wang, Y.-T. Chen, H.-Z. Wang, C.-Y. Su, W. Wang, *J. Am. Chem. Soc.* **2016**, *138*, 3031–3037.

[76] X. Yan, P. Li, X. Song, J. Li, B. Ren, S. Gao, R. Cao, *Coord. Chem. Rev.* **2021**, *443*, 214034.

[77] P. Yang, Y. Shu, Q. Zhuang, Y. Li, J. Gu, *Chem. Commun.* **2019**, *55*, 12972–12975.

[78] S. Lee, G. Barin, C. M. Ackerman, A. Muchenditsi, J. Xu, J. A. Reimer, S. Lutsenko, J. R. Long, C. J. Chang, *J. Am. Chem. Soc.* **2016**, *138*, 7603–7609.

[79] F.-Z. Cui, R.-R. Liang, Q.-Y. Qi, G.-F. Jiang, X. Zhao, *Adv. Sustainable Syst.* **2019**, *3*, 1800150.

[80] a) X. Shen, S. Ma, H. Xia, Z. Shi, Y. Mu, X. Liu, *J. Mater. Chem. A* **2018**, *6*, 20653–20658; b) S. Jiao, L. Deng, X. Zhang, Y. Zhang, K. Liu, S. Li, L. Wang, D. Ma, *ACS Appl. Mater. Interfaces* **2021**, *13*, 39404–39413.

[81] X. Li, L. Jin, L. Huang, X. Ge, H. Deng, H. Wang, Y. Li, L. Chai, S. Ma, *J. Environ. Chem. Eng.* **2021**, *9*, 106357.

[82] H. Kaur, S. Sinha, V. Krishnan, R. R. Koner, *Ind. Eng. Chem. Res.* **2020**, *59*, 8538–8550.

[83] a) C. W. Abney, R. T. Mayes, T. Saito, S. Dai, *Chem. Rev.* **2017**, *117*, 13935–14013; b) N. Tang, J. Liang, C. Niu, H. Wang, Y. Luo, W. Xing, S. Ye, C. Liang, H. Guo, J. Guo, Y. Zhang, G. Zeng, *J. Mater. Chem. A* **2020**, *8*, 7588–7625.

[84] a) B. Li, Q. Sun, Y. Zhang, C. W. Abney, B. Aguila, W. Lin, S. Ma, *ACS Appl. Mater. Interfaces* **2017**, *9*, 12511–12517; b) B. Aguila, Q. Sun, H. Cassady, C. W. Abney, B. Li, S. Ma, *ACS Appl. Mater. Interfaces* **2019**, *11*, 30919–30926.

[85] Q. Sun, B. Aguila, J. Perman, A. S. Ivanov, V. S. Bryantsev, L. D. Earl, C. W. Abney, L. Wojtas, S. Ma, *Nat. Commun.* **2018**, *9*, 1644.

[86] Q. Sun, Y. Song, B. Aguila, A. S. Ivanov, V. S. Bryantsev, S. Ma, *Adv. Sci.* **2021**, *8*, 2001573.

[87] Y. Sonh, C. Zhu, Q. Sun, B. Aguila, C. W. Abney, L. Wojtas, S. Ma, *ACS Cent. Sci.* **2021**, *7*, 1650–1656.

[88] Q. Sun, B. Aguila, L. D. Earl, C. W. Abney, L. Wojtas, P. K. Thallapally, S. Ma, *Adv. Mater.* **2018**, *30*, 1705479.

[89] a) W.-R. Cui, C.-R. Zhang, W. Jiang, F.-F. Li, R.-P. Liang, J. Liu, J.-D. Qiu, *Nat. Commun.* **2020**, *11*, 436; b) F.-F. Li, W.-R. Cui, W. Jiang, C.-R. Zhang, R.-P. Liang, J.-D. Qiu, *J. Hazard. Mater.* **2020**, *392*, 122333; c) W.-R. Cui, F.-F. Li, R.-H. Xu, C.-R. Zhang, X.-R. Chen, R.-H. Yan, R.-P. Liang, J.-D. Qiu, *Angew. Chem. Int. Ed.* **2020**, *59*, 17684–17690; *Angew. Chem.* **2020**, *132*, 17837–17843.

[90] a) Y. Yuan, Y. Yang, X. Ma, Q. Meng, L. Wang, S. Zhao, G. Zhu, *Adv. Mater.* **2018**, *30*, 1706507; b) Z. Wang, R. Ma, Q. Meng, Y. Yang, X. Ma, X. Ruan, Y. Yuan, G. Zhu, *J. Am. Chem. Soc.* **2021**, *143*, 14523–14529; c) Z. Li, Q. Meng, Y. Yang, X. Zou, Y. Yuan, G. Zhu, *Chem. Sci.* **2020**, *11*, 4747–4752; d) Y. Yuan, Q. Meng, M. Faheem, Y. Yang, Z. Li, Z. Wang, D. Deng, F. Sun, H. He, Y. Huang, H. Sha, G. Zhu, *ACS Cent. Sci.* **2019**, *5*, 1432–1439; e) Z. Wang, Q. Meng, R. Ma, Z. Wang, Y. Yang, H. Sha, X. Ma, X. Ruan, X. Zou, Y. Yuan, G. Zhu, *Chem* **2020**, *6*, 1683–1691.

[91] a) H. Zhang, W. Liu, A. Li, D. Zhang, X. Li, F. Zhai, L. Chen, L. Chen, Y. Wang, S. Wang, *Angew. Chem. Int. Ed.* **2019**, *58*, 16110–16114; *Angew. Chem.* **2019**, *131*, 16256–16260; b) H. Li, F. Zhai, D. Gui, X. Wang, C. Wu, D. Zhang, X. Dai, H. Deng, X. Su, J. Diwu, Z. Lin, Z. Chai, S. Wang, *Appl. Catal. B* **2019**, *254*, 47–54.

[92] a) B. Li, Y. Zhang, D. Ma, Z. Xing, T. Ma, Z. Shi, X. Ji, S. Ma, *Chem. Sci.* **2016**, *7*, 2138–2144; b) D. Banerjee, S. K. Elsaidi, B. Aguila, B. Li, D. Kim, M. J. Schweiger, A. A. Kruger, C. J. Doonan, S. Ma, P. K. Thallapally, *Chem. Eur. J.* **2016**, *22*, 17581–17584.

[93] Q. Sun, L. Zhu, B. Aguila, P. K. Thallapally, C. Xu, J. Chen, S. Wang, D. Rogers, S. Ma, *Nat. Commun.* **2019**, *10*, 1646.

[94] a) J. Li, X. Dai, L. Zhu, C. Xu, D. Zhang, M. A. Silver, P. Li, L. Chen, Y. Li, D. Zuo, H. Zhang, C. Xiao, J. Chen, J. Diwu, O. K. Farha, T. E. Albrecht-Schmitt, Z. Chai, S. Wang, *Nat. Commun.* **2018**, *9*, 3007; b) J. Li, B. Li, N. Shen, L. Chen, Q. Guo, L. Chen, L. He, X. Dai, Z. Chai, S. Wang, *ACS Cent. Sci.* **2021**, *7*, 1441–1450; c) J. Li, L. Chen, N. Shen, R. Xie, M. V. Sheridan, X. Chen, D. Sheng, D. Zhang, Z. Chai, S. Wang, *Sci. China Chem.* **2021**, *64*, 1251–1260.

[95] L. Zhu, D. Sheng, C. Xu, X. Dai, M. A. Silver, J. Li, P. Li, Y. Wang, Y. Wang, L. Chen, C. Xiao, J. Chen, R. Zhou, C. Zhang, O. K. Farha, Z. Chai, T. E. Albrecht-Schmitt, S. Wang, *J. Am. Chem. Soc.* **2017**, *139*, 14873–14876.

[96] L. He, S. Liu, L. Chen, X. Dai, J. Li, M. Zhang, F. Ma, C. Zhang, Z. Yang, R. Zhou, Z. Chai, S. Wang, *Chem. Sci.* **2019**, *10*, 4293–4305.

[97] Y. Bai, L. Chen, L. He, B. Li, L. Chen, F. Wu, L. Chen, M. Zhang, Z. Liu, Z. Chai, S. Wang, *Chem* **2022**, *8*, 1442–1459.
[98] T. Geng, S. Ye, Z. Zhu, W. Zhang, *J. Mater. Chem. A* **2018**, *6*, 2808–2816.
[99] P. Wang, Q. Xu, Z. Li, W. Jiang, Q. Jiang, D. Jiang, *Adv. Mater.* **2018**, *30*, 1801991.
[100] Z. Yan, Y. Yuan, Y. Tian, D. Zhang, G. Zhu, *Angew. Chem. Int. Ed.* **2015**, *54*, 12733–12737; *Angew. Chem.* **2015**, *127*, 12924–12928.

Manuscript received: November 13, 2022
Accepted manuscript online: December 20, 2022
Version of record online: January 12, 2023